Run-2 Higgs Couplings from ATLAS

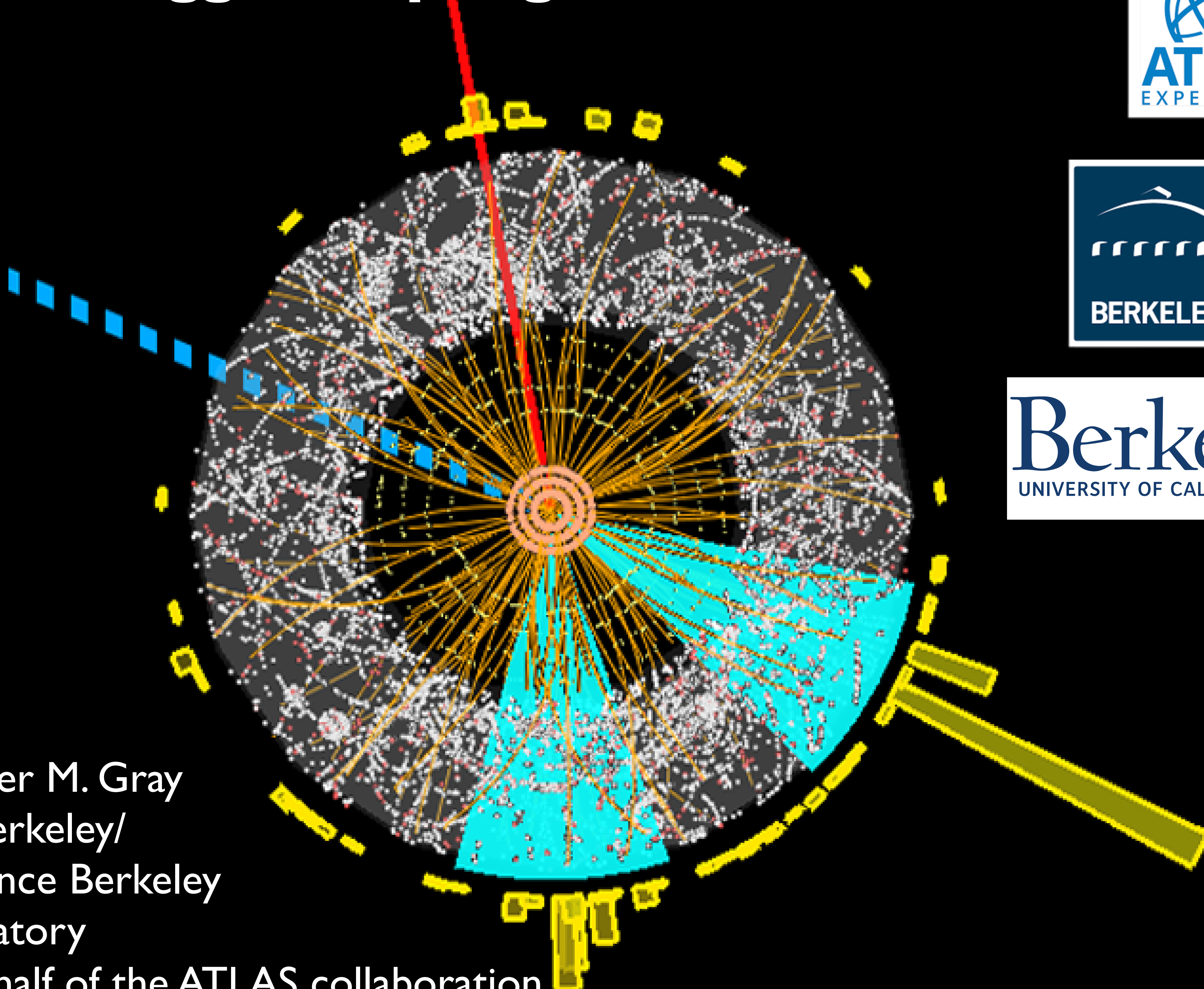

Heather M. Gray
UC Berkeley/
Lawrence Berkeley
Laboratory
on behalf of the ATLAS collaboration

The Higgs and the LHC

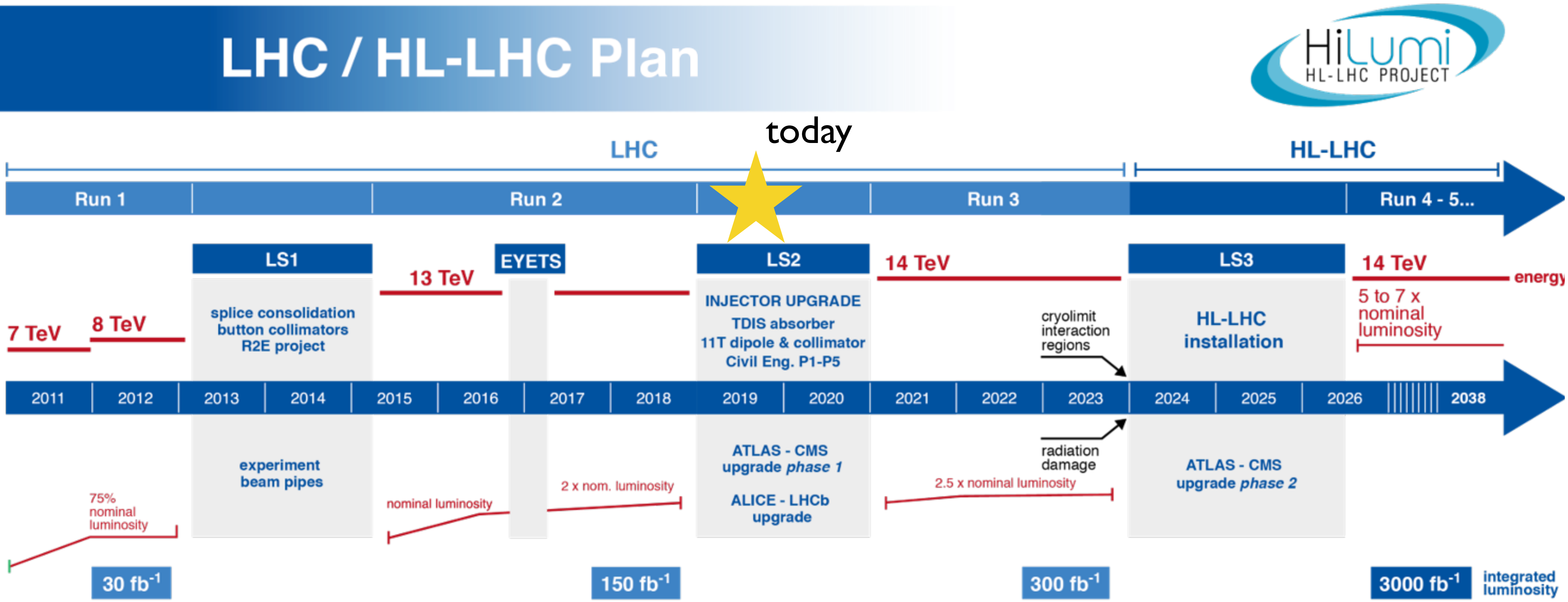

First beam in ATLAS (2009)

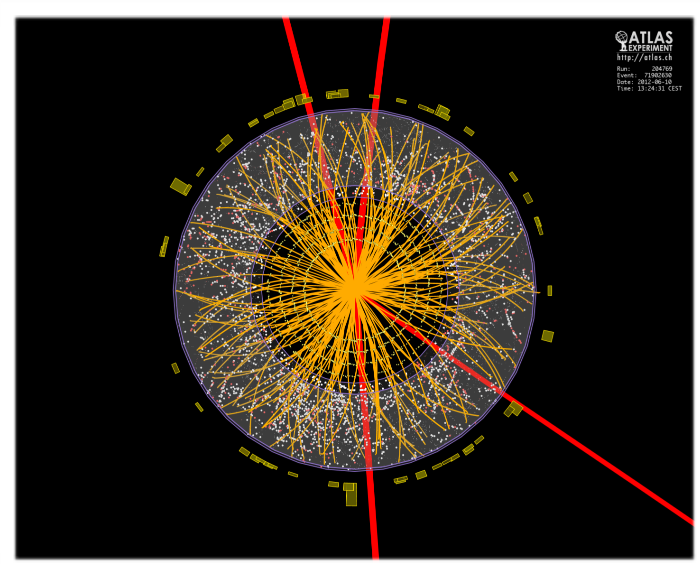

Higgs discovery (2012)

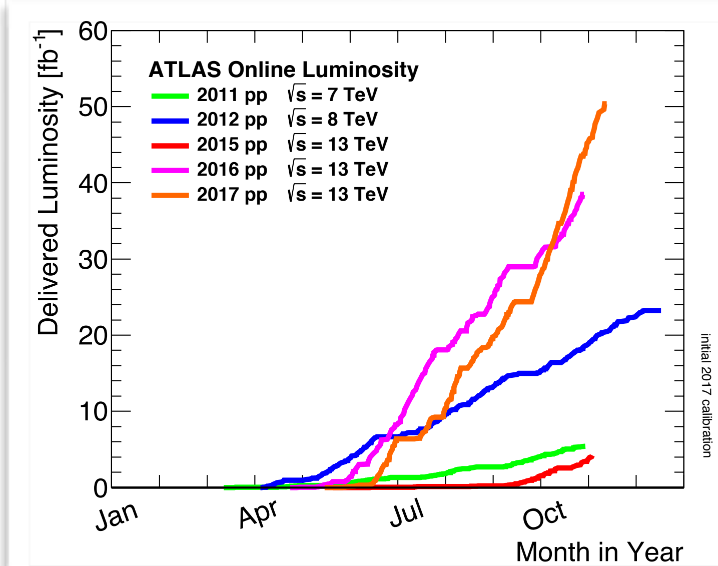

Only ~5% of total expected data

Higgs Properties

- Mass: 124.97 ± 0.24 GeV
- (Indirect) width: < 14.4 MeV
  - (15.2 MeV)
- Spin and parity $J^{PC} = 0^{++}$
- Couplings

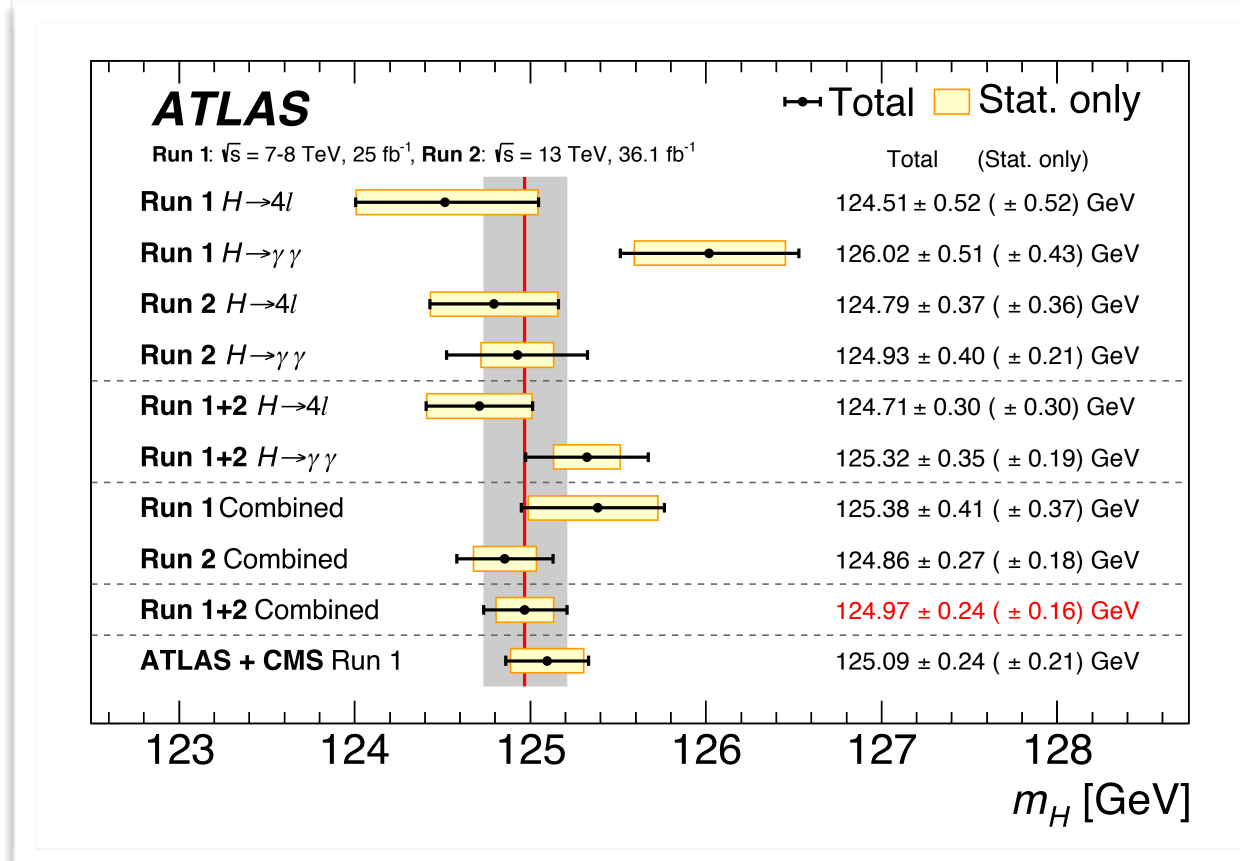

PLB784 (2018) 345

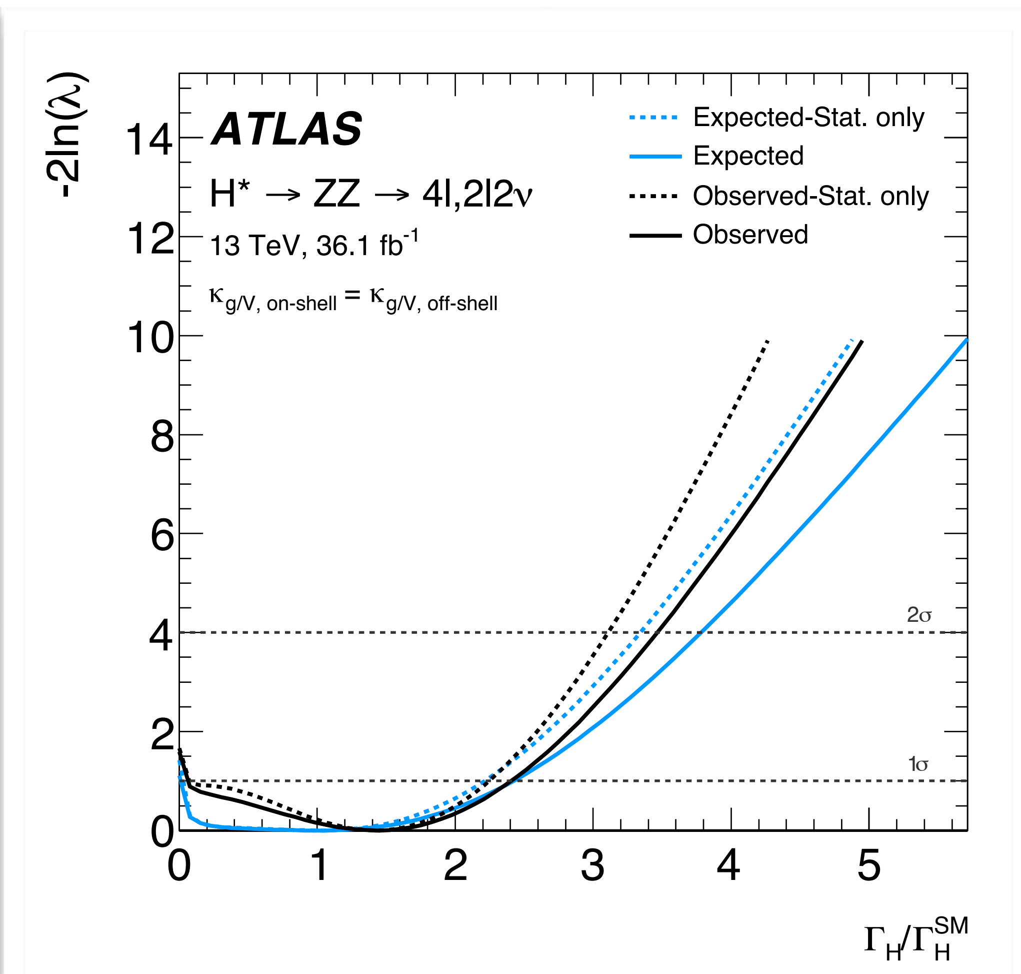

PLB786 (2018) 223

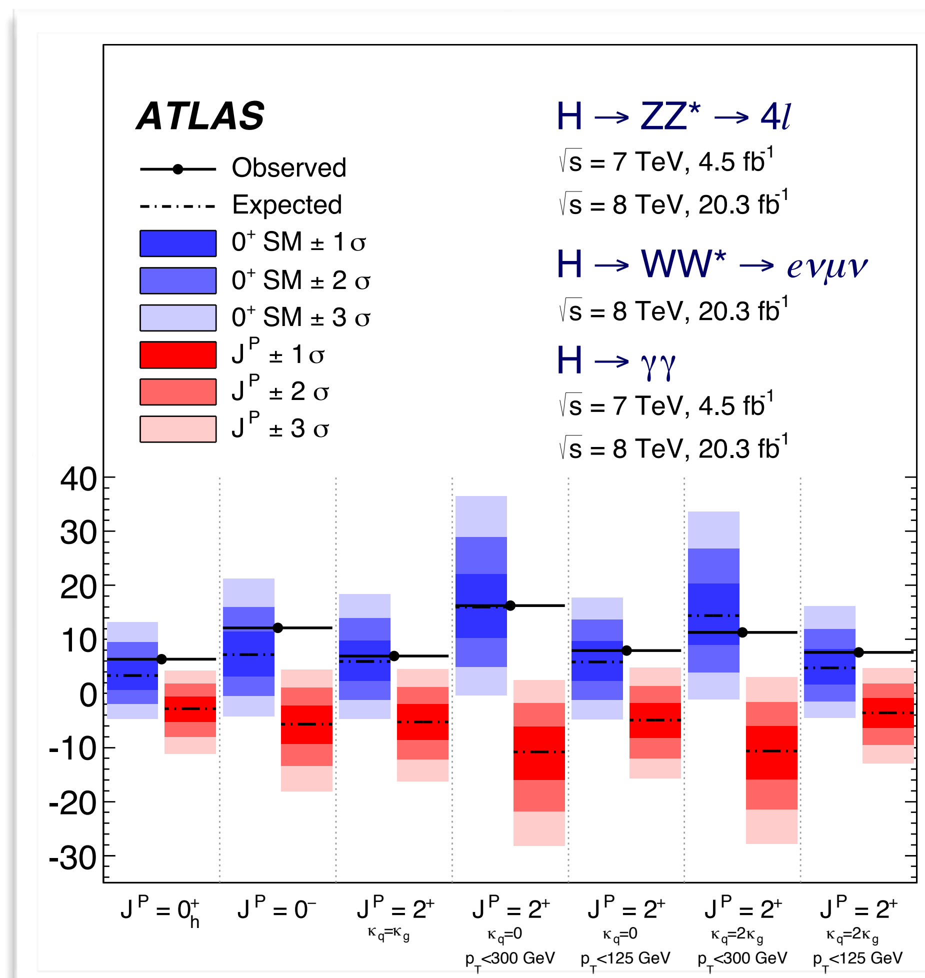

EPJC75 (2015) 476

Probing Higgs Couplings at the LHC

σ [pb]
#Higgs produced during Run-2

4 main production modes

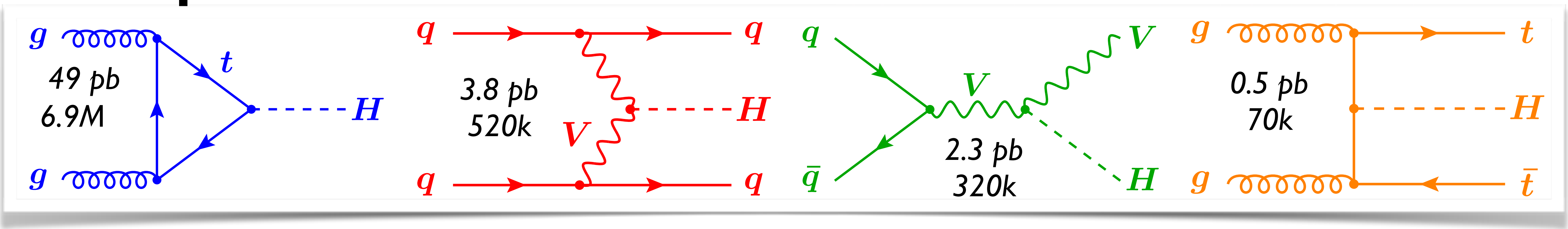

Main production channel: gluon-gluon fusion

2 forward jets, little central hadronic activity

Tag W and Z decays

Tag 2 top quarks

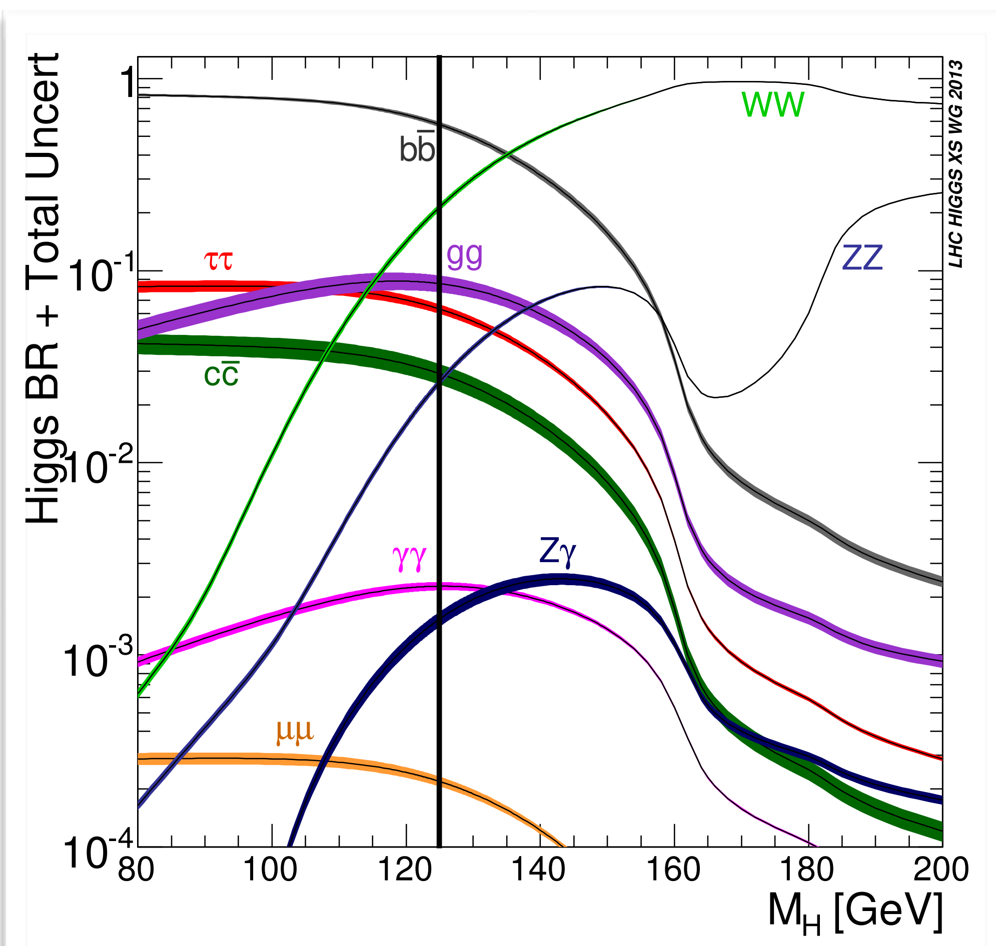

5 key decay channels

- H→bb: 58 %
- H→WW*: 21%
- H→τ⁺τ⁻: 6.3%
- H→ZZ*: 2.6%
- H→γγ: 0.23%

Decay branching fractions for m_H = 125 GeV

Recent ATLAS Higgs coupling results

- **Results with 80 fb-1**
  - VH(bb): PLB 786 (2018) 59
  - ttH: PLB 784 (2018) 173 NEW
  - H(γγ): ATLAS-CONF-2019-005, ATLAS-CONF-2018-028
  - H(ZZ→4l): ATLAS-CONF-2019-005, ATLAS-CONF-2018-018
  - H(μμ): ATLAS-CONF-2019-005, ATLAS-CONF-2018-026
  - λ_{HHH}: ATL-PHYS-PUB-2019-009 NEW
- **Results with 36 fb-1**
  - H(ττ): arXiv:1811.08856
  - ttH(ML): PRD 97 (2018) 072003
  - ttH(bb): PRD 97 (2018) 072016
  - VBF H(bb): PRD 98 (2018) 052003
  - H(inv): ATLAS-CONF-2018-054
  - H(WW): PLB 789 (2019) 508

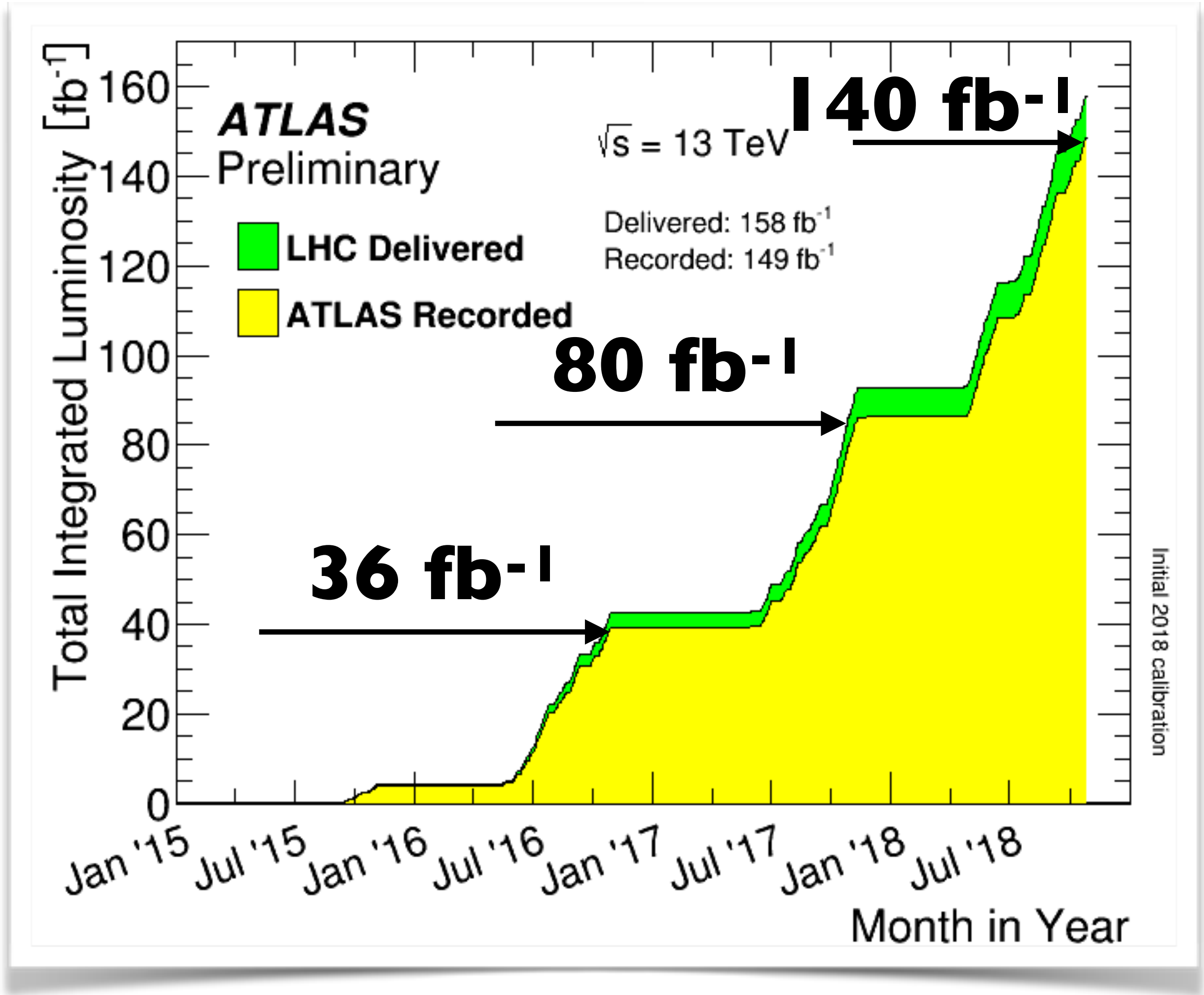

Discovery Channels: H→γγ and H→ZZ→4l

- Results using 80 fb^{-1}
- Probing cross-sections of individual production modes
  - Up to ~15% precision
- Exp. and theo. systematics play a key role

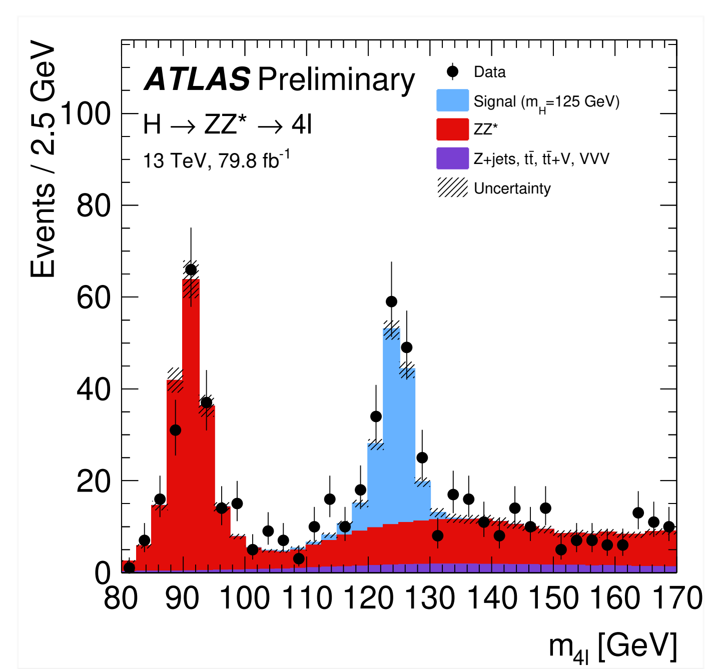

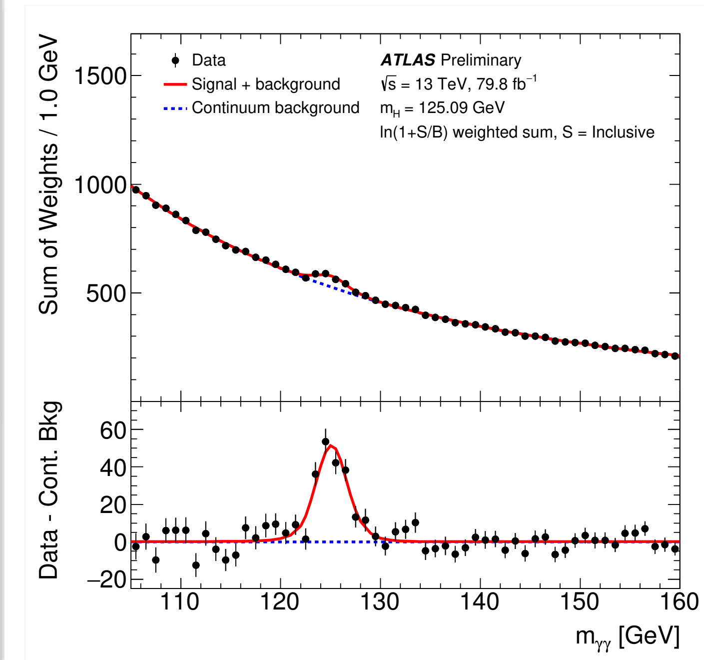

ATLAS-CONF-2018-028, ATLAS-CONF-2018-018

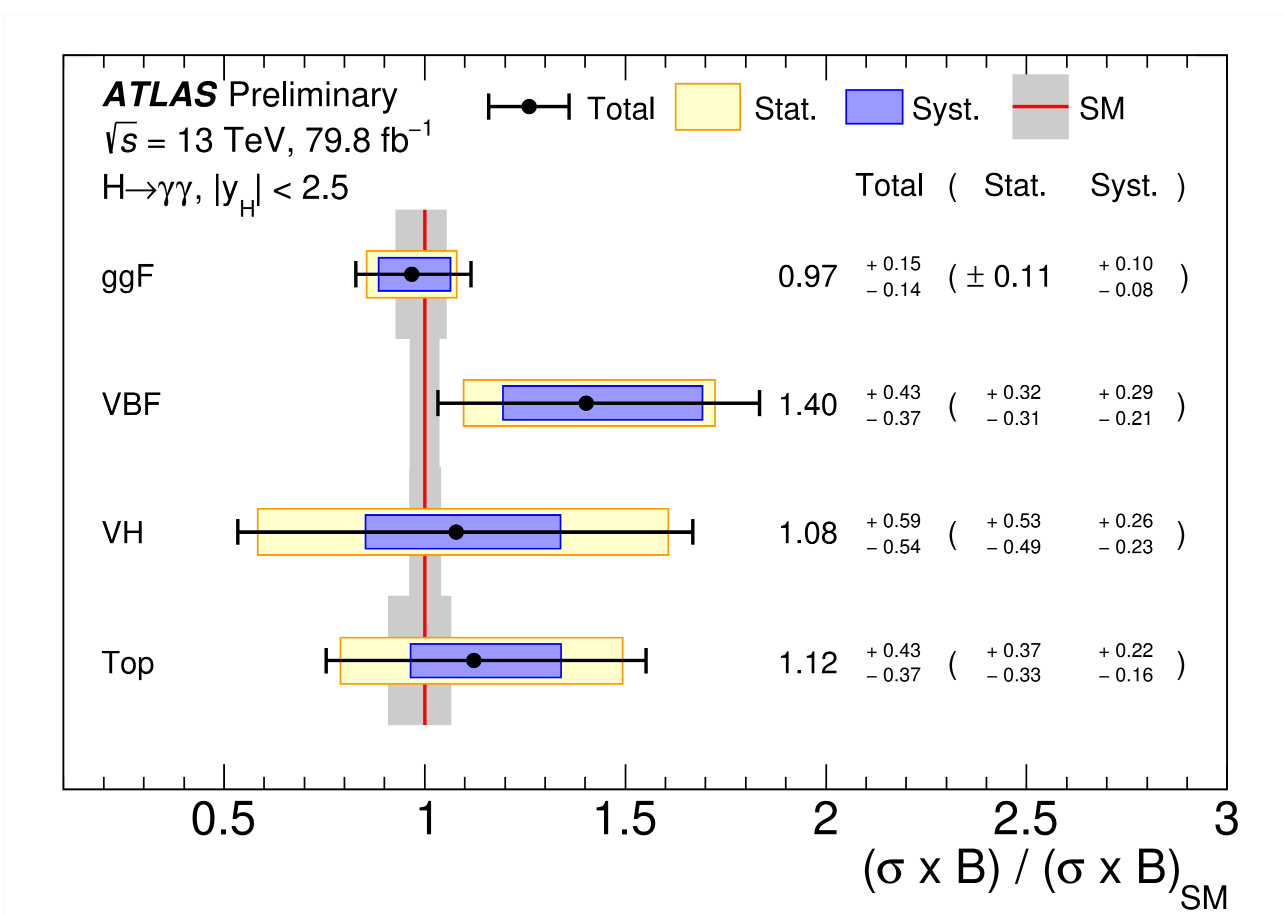

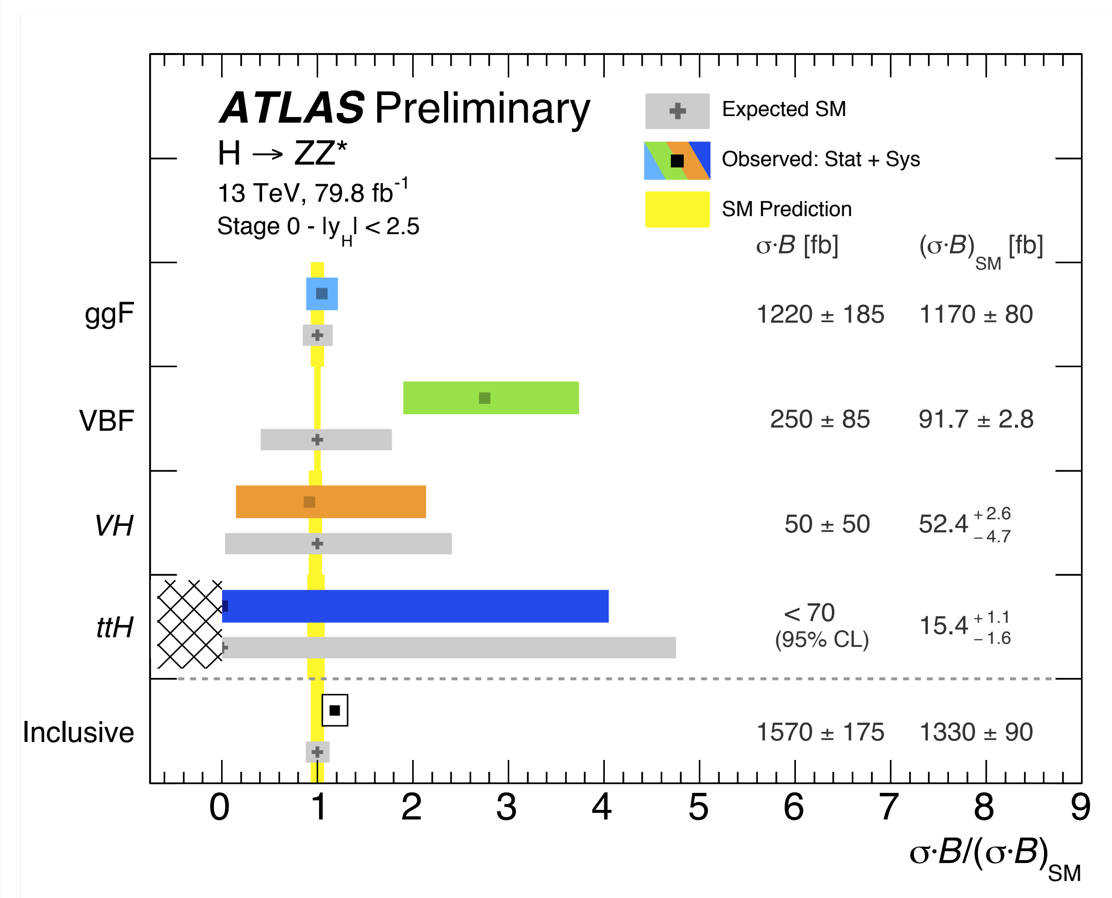

See talk by F. Cerutti, e.g. for simplified template cross-section (STXS) results

Measurements with H→WW

- Cross-section x BR measurements for ggF and VBF production
- ggF: $11.4^{+1.2}_{-1.1}$(stat)$^{+1.2}_{-1.1}$(theo syst.)$^{+1.4}_{-1.3}$ (exp syst.) pb
  - (10.4 ± 0.6 pb)
- VBF: $0.5^{+0.24}_{-0.22}$ (stat) ± 0.10 (theo syst.)$^{+0.12}_{-0.13}$(exp syst.) pb
  - (0.81 ± 0.02 pb)

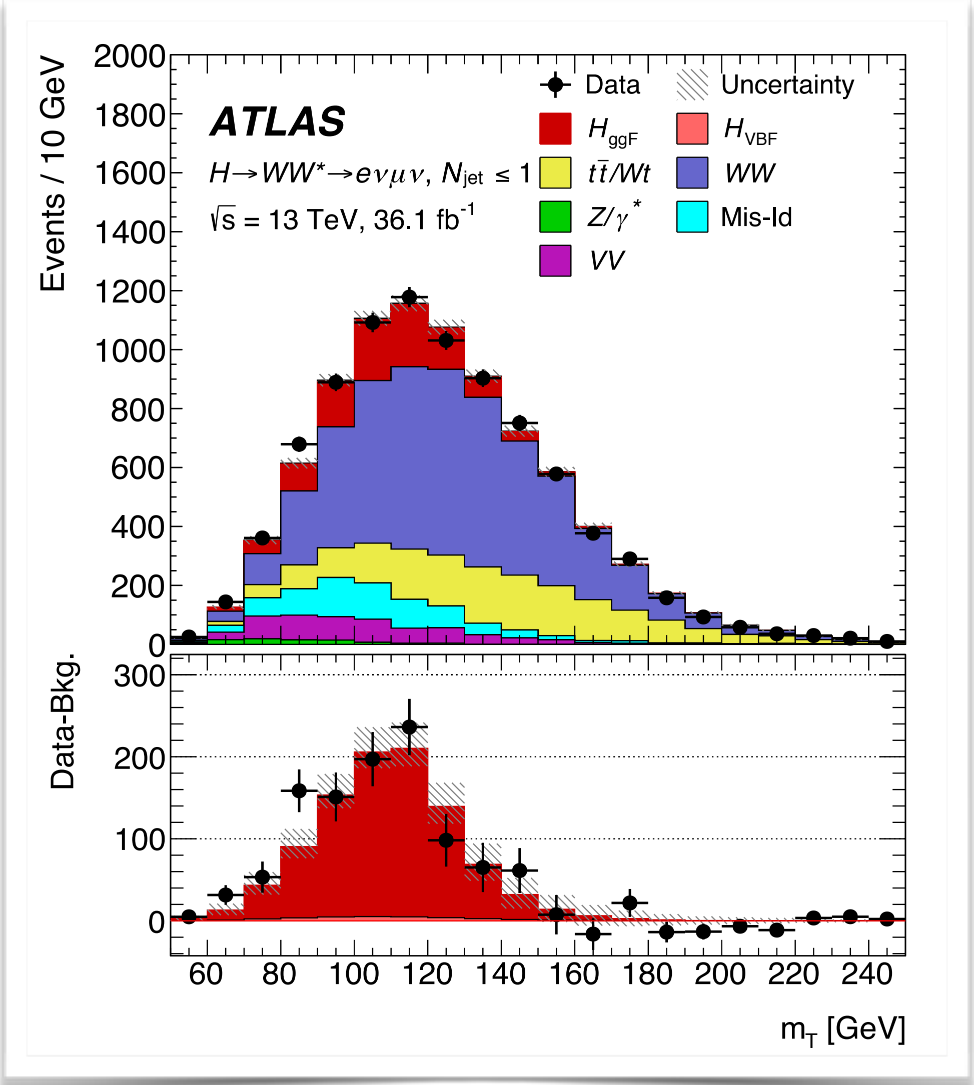

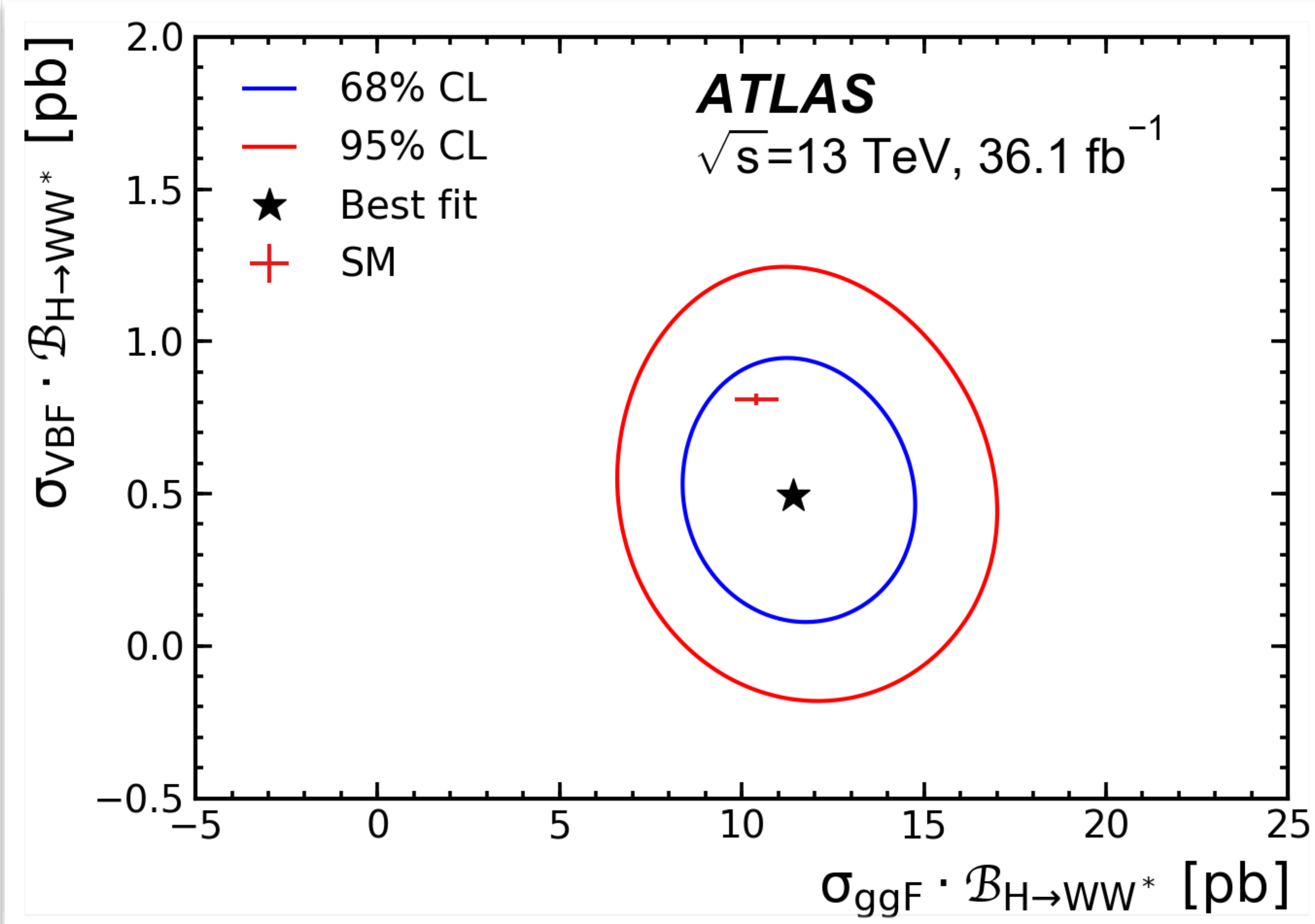

PLB 789 (2019) 508

Observation of coupling to τ-leptons

- 5.5 (5.0)σ for H→ττ (ATLAS/CMS Run-1)
- 6.4 (5.4)σ from ATLAS (7-13 TeV results)
- Sensitive decay channel for VBF production
  - ggF: 3.1 ± 0.1(stat) $^{+0.1.6}_{-1.3}$ (syst.) pb
    - (SM: 3.05 ± 0.13 pb)
  - VBF:0.28 ± 0.09 (stat)$^{+0.11}_{-0.9}$ (syst.) pb
    - (SM: 0.237 ± 0.006 pb)

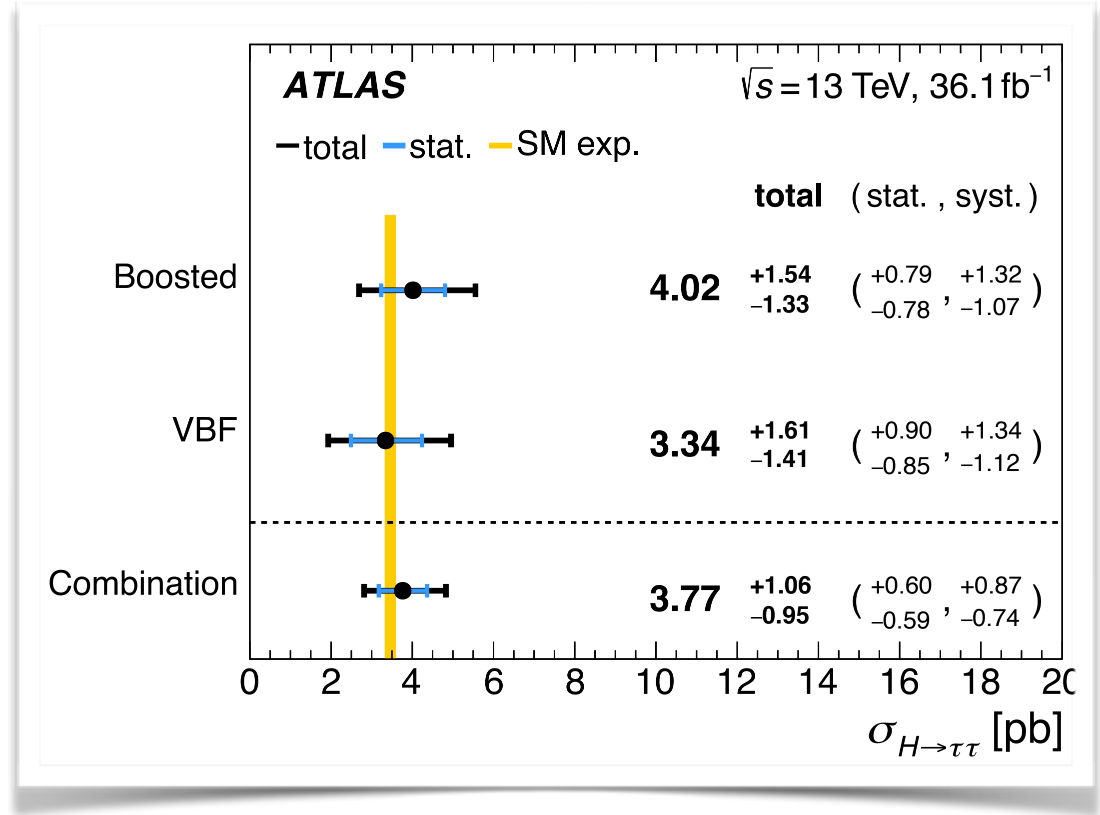

JHEP08(2016)045, arXiv:1811.08856

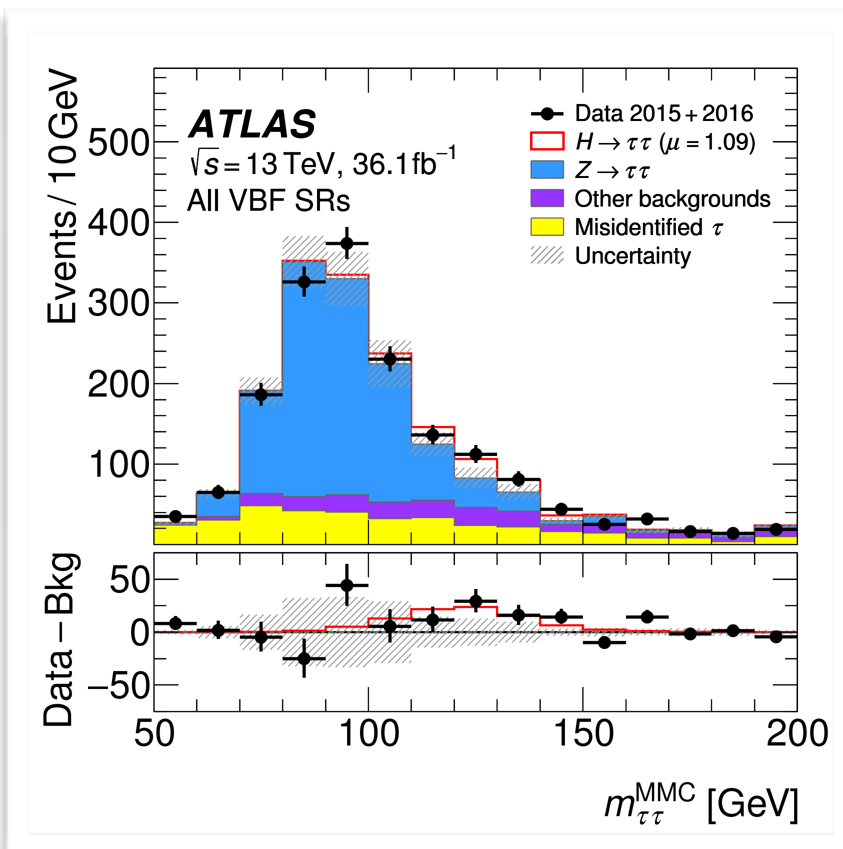

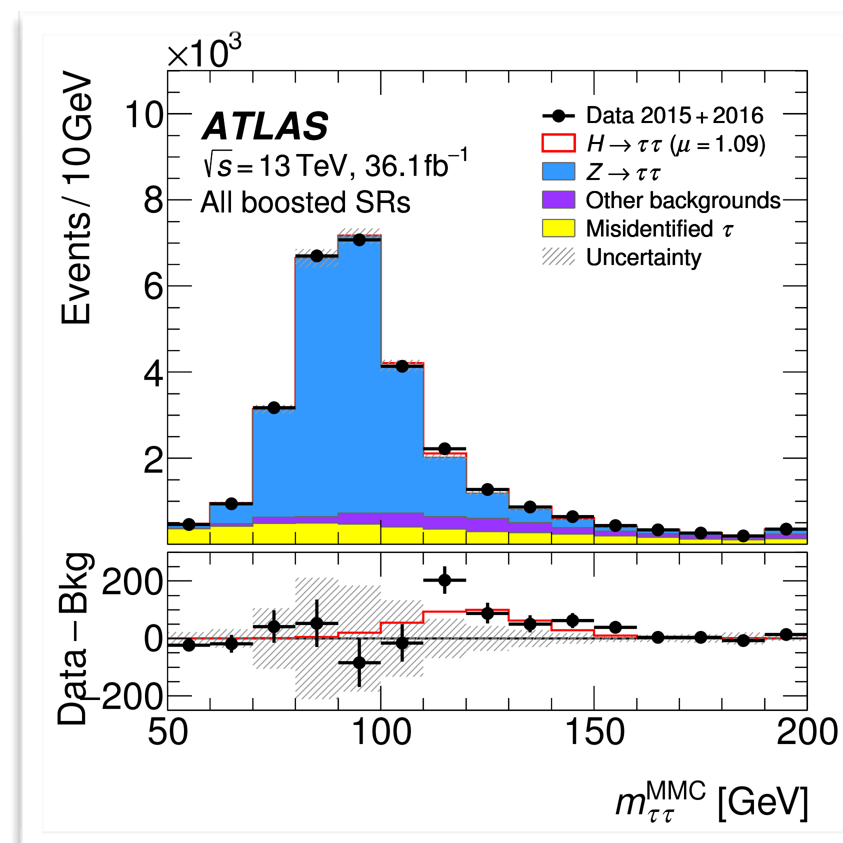

Observation of coupling to b-quarks

VH

- Difficult channel despite the large branching ratio (58%) due to large backgrounds
- Most sensitive production mode: VH production
- Further searches using ggF, VBF and ttH production
- Observed with 5.4σ (5.5σ) by ATLAS
- Cross-checked via observation of VZ(bb) production
- Most sensitive channel for VH production

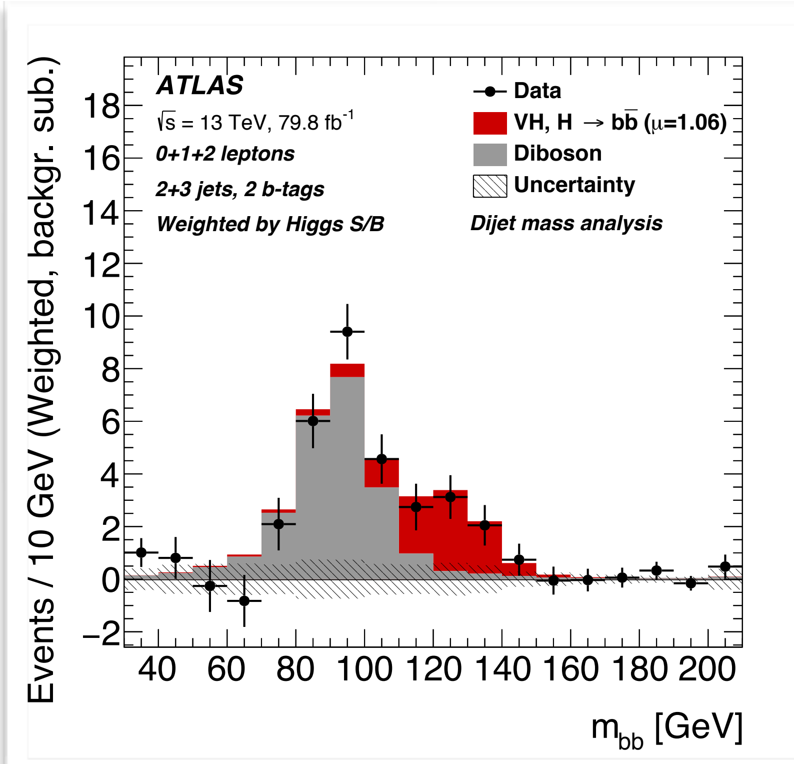

VH

PLB 786 (2018) 59

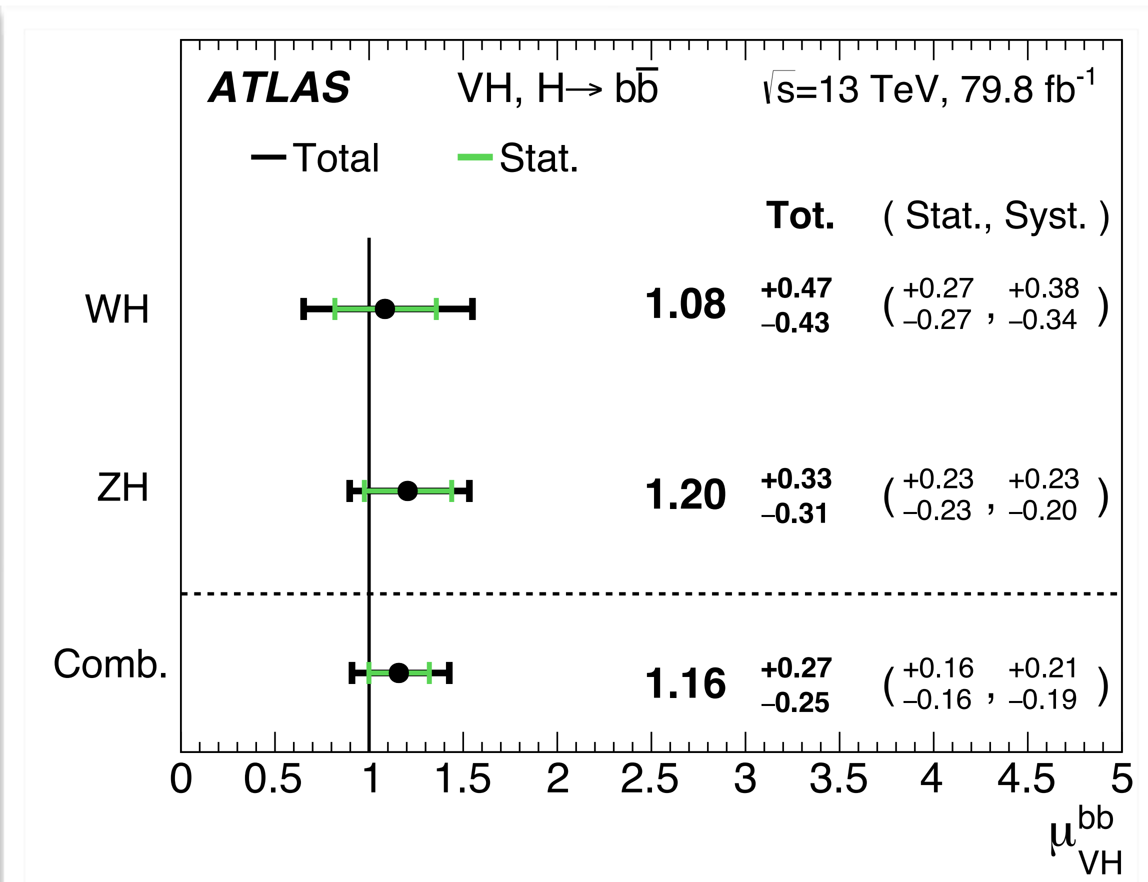

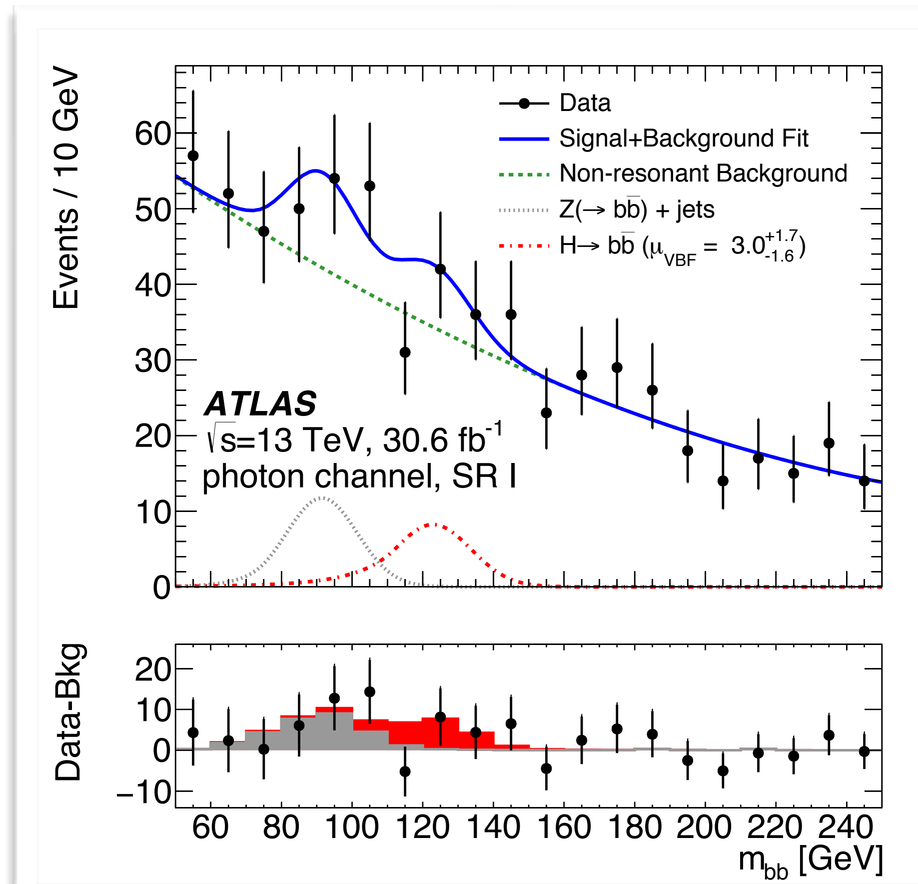

VBF

PRD 98 (2018) 052003

Observation of coupling to top quarks

See talk by J. Dickinson

- ttH production provides a direct probe of the coupling of the Higgs boson to top quarks
  - Probes potential new physics contribution in the ggF loop
- 6.3σ (5.1σ) observation for ttH production from ATLAS through the combination of the major decay modes

Combination

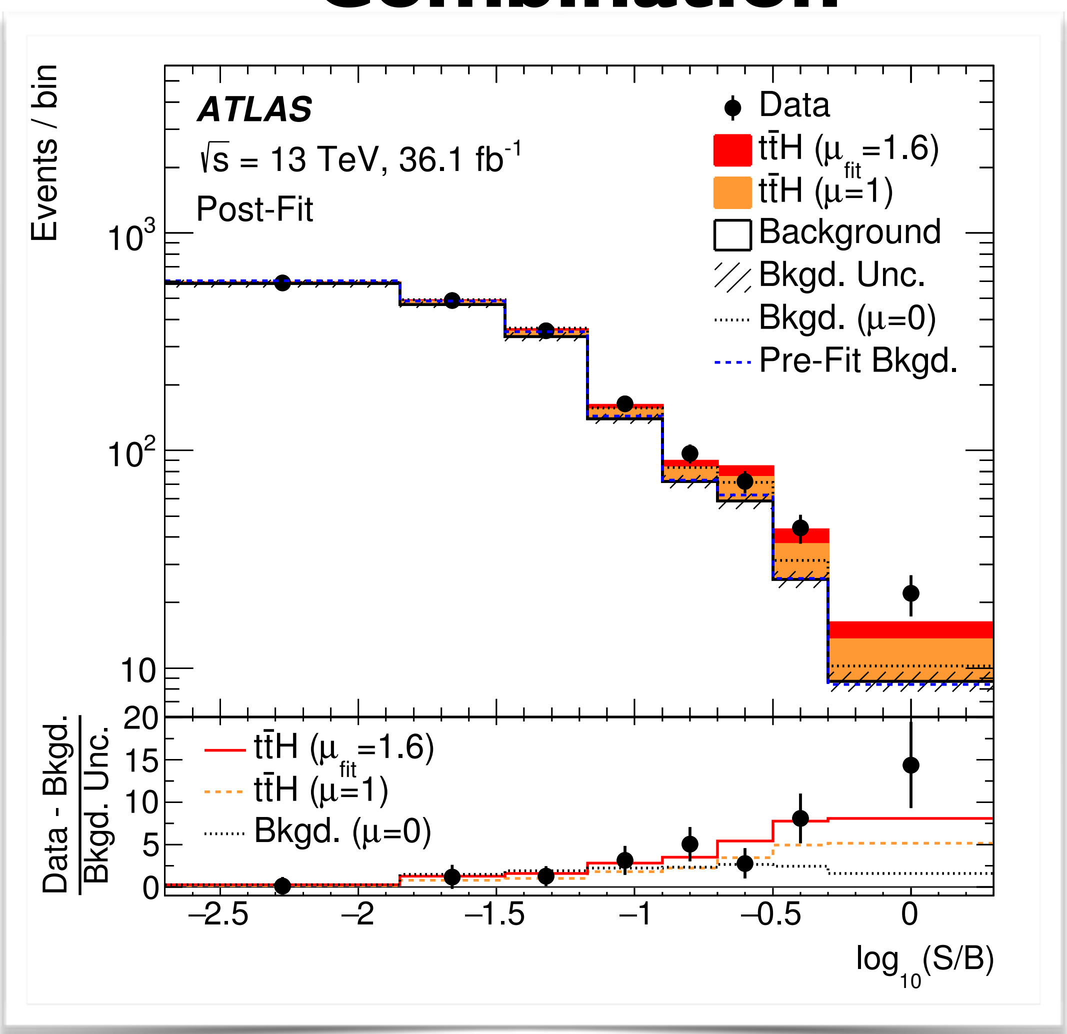

PRD 97 (2018) 072003

ttH(γγ)

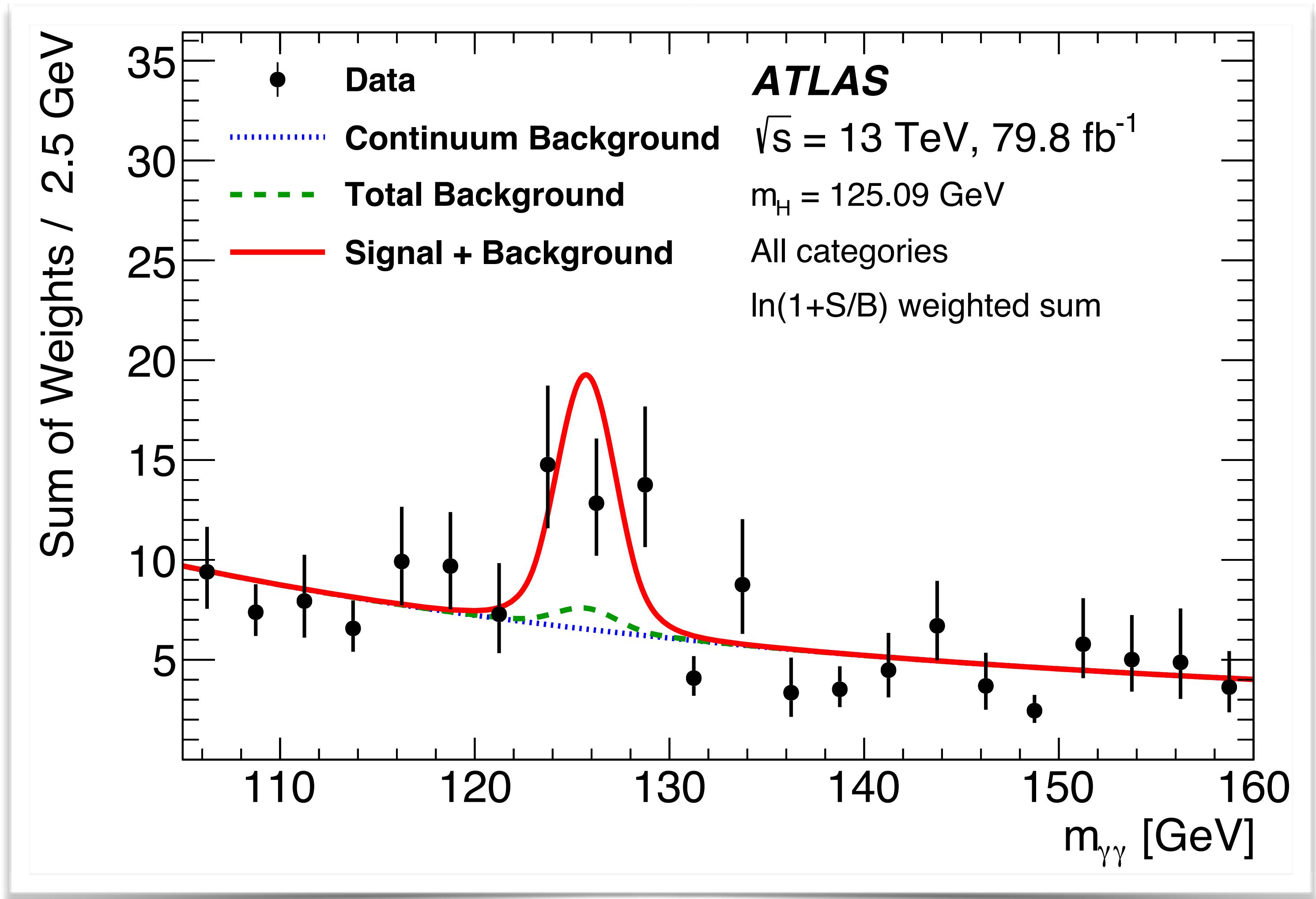

PLB 784 (2018) 173

Rare Higgs decays

- Exploit growing LHC dataset to add limits on further decay channels
  - H→μμ: < 2.1 (2.0) x SM
  - H→Zγ: < 6.6 (4.4) x SM
  - H→cc:
    - < ZH(cc):110 x SM
    - < J/ψγ: 120 x SM
  - H→φγ: < 200 x SM; H→ργ: < 50 x SM

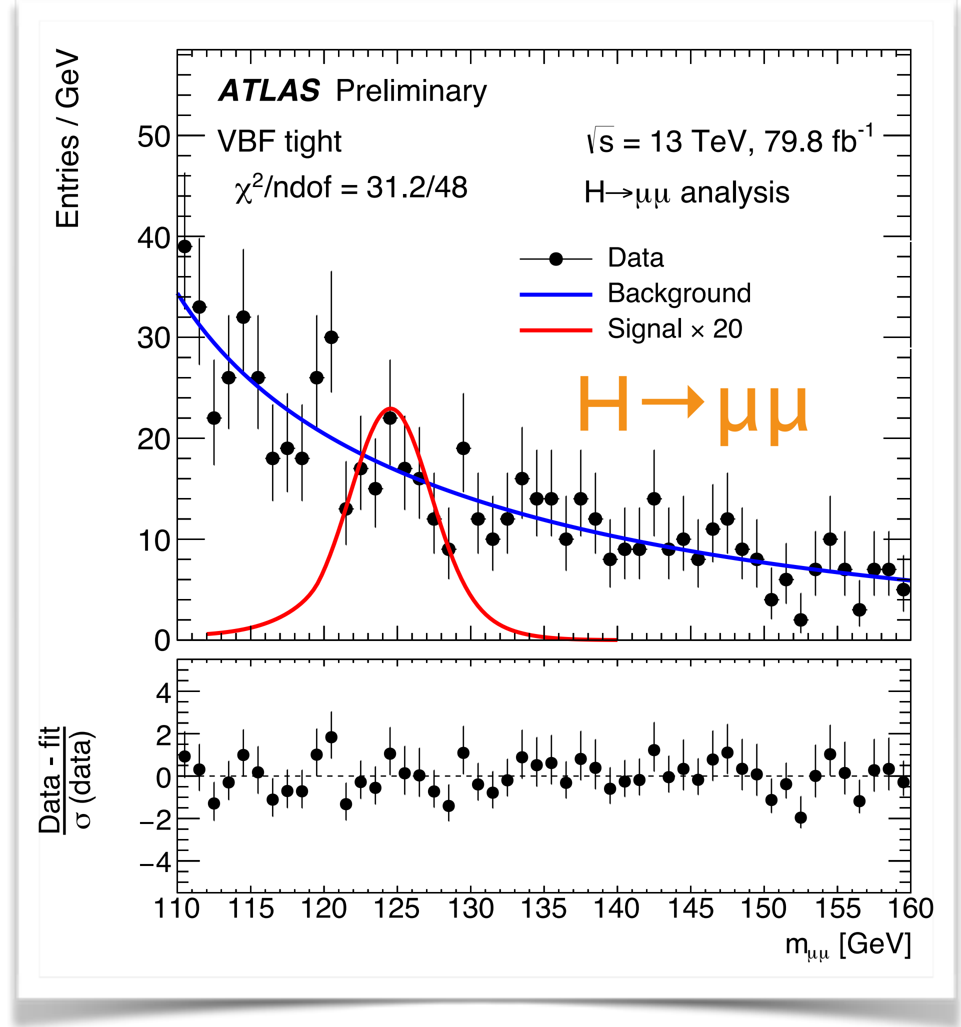

ATLAS-CONF-2018-026

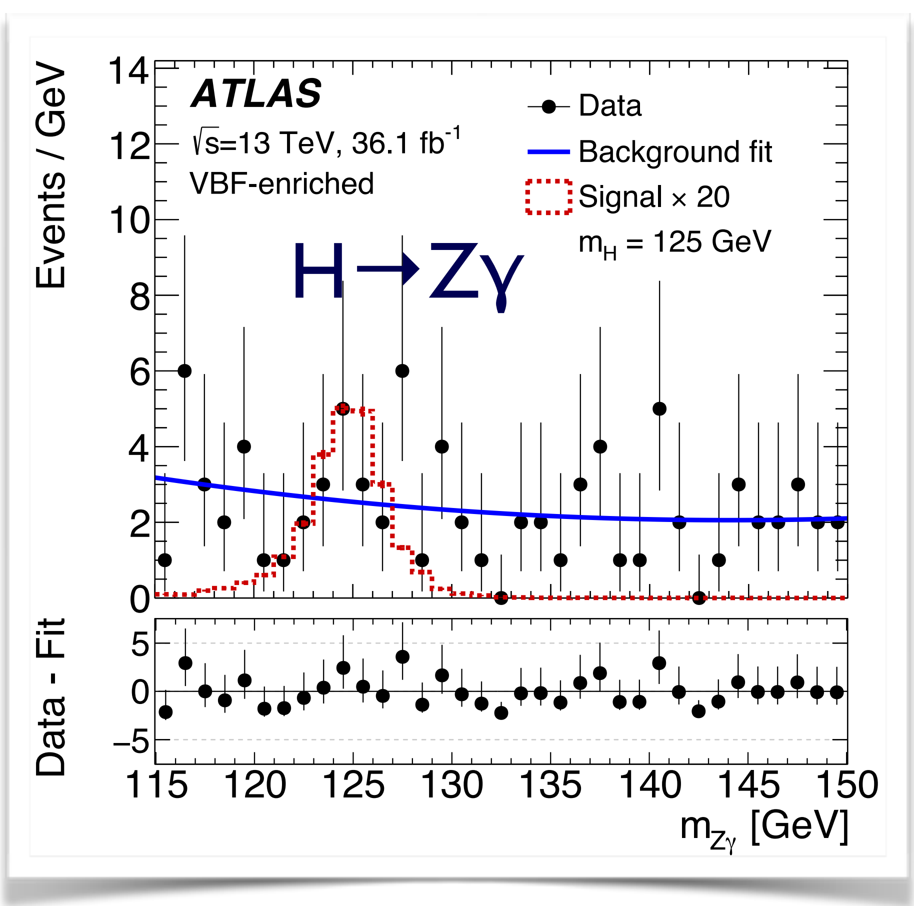

JHEP 10 (2017) 112

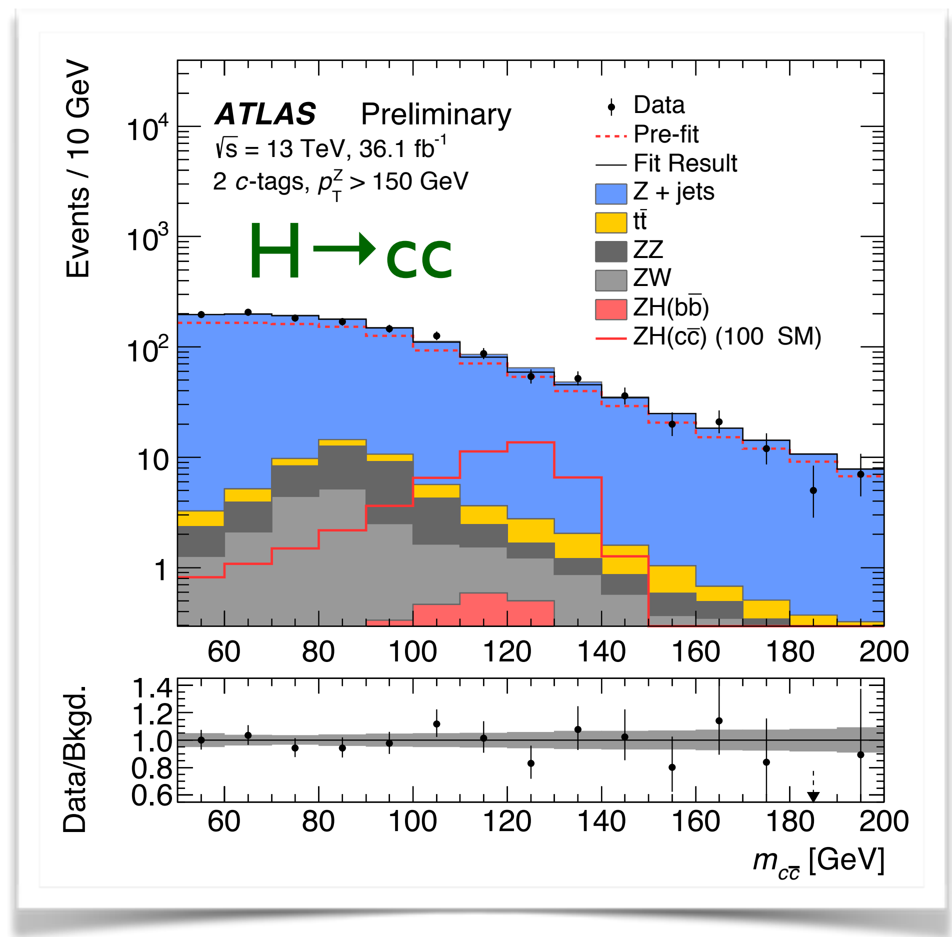

PRL 120 (2018) 211802

Higgs to Invisible

- Indirect: constraints from coupling fits
- Direct: searches for Higgs to decays to invisible particles
  - Three separate ATLAS searches: V(had)H(inv), Z(lep)H(inv), VBF H(inv)
  - $B(H \rightarrow inv) < 0.26\ (0.17^{+0.07}_{-0.05})$ @ 95% CL

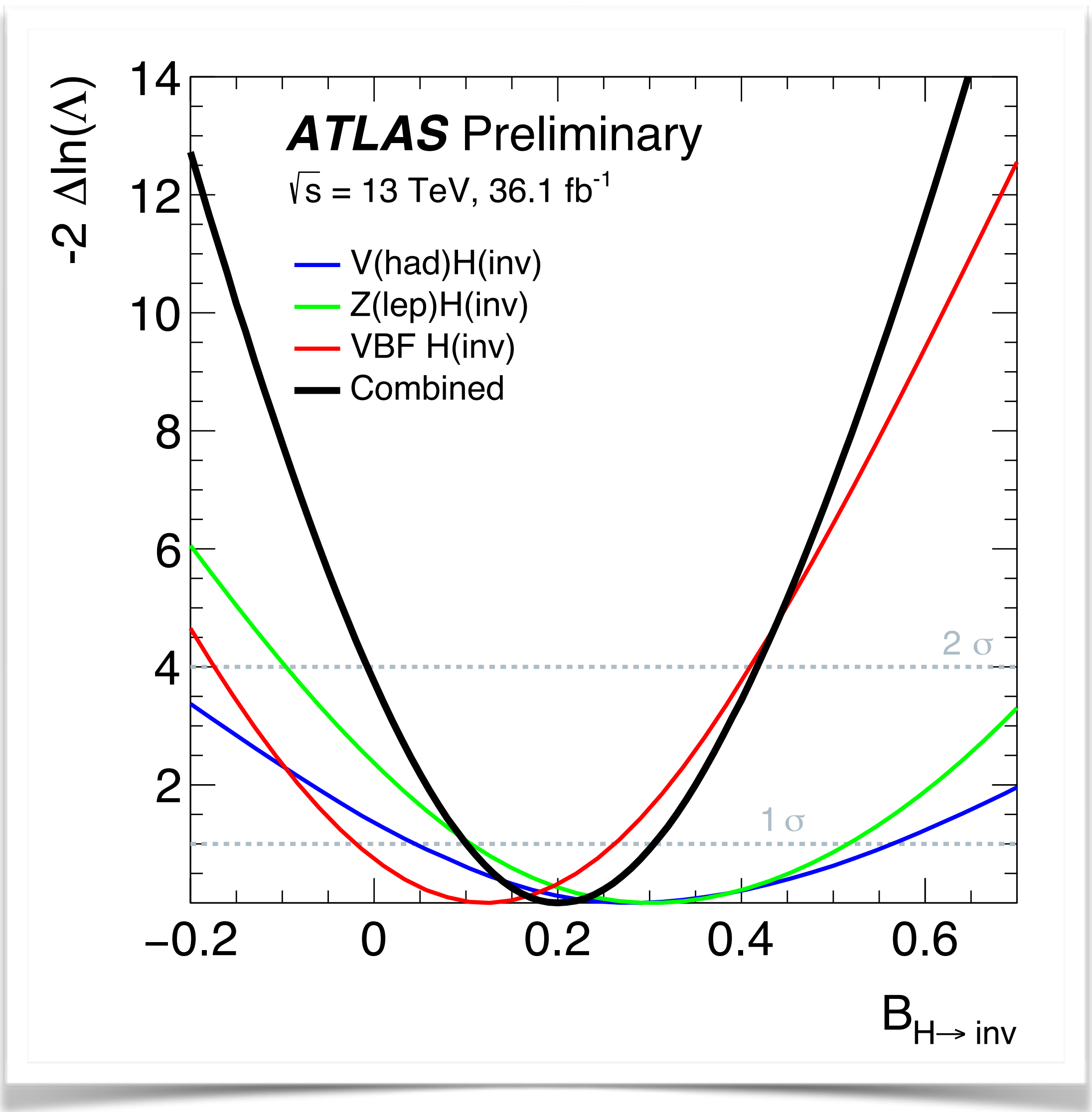

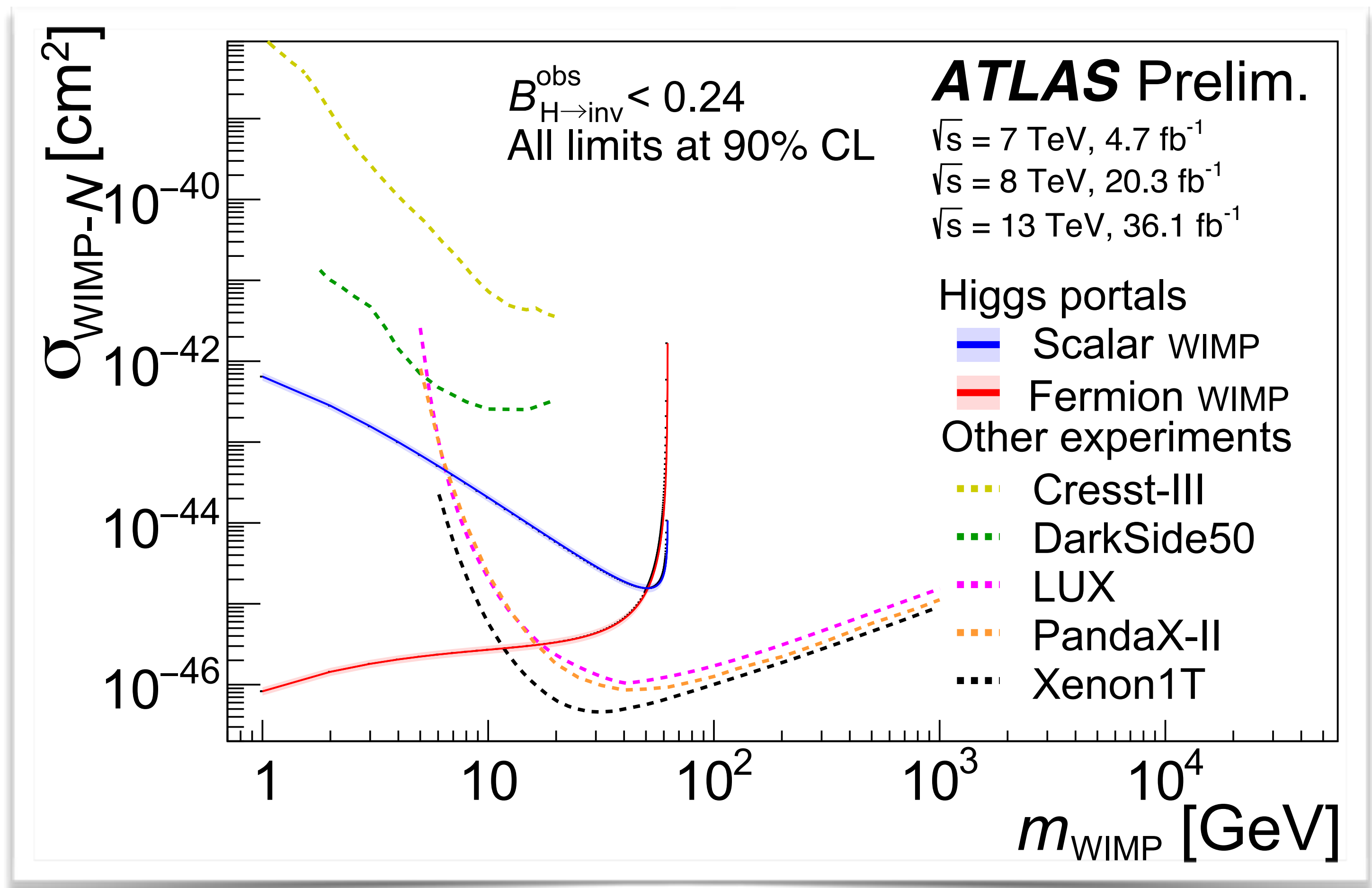

ATLAS-CONF-2018-054, arXiv:0605188

ATLAS combination

NEW

	$H\to\gamma\gamma$	$H \to ZZ^*$	$H \to WW^*$	$H \to \tau\tau$	$H \to b\bar{b}$
$t\bar{t}H$	$t\bar{t}H$ leptonic (3 categories) $t\bar{t}H$ hadronic (4 categories)	$t\bar{t}H$ multilepton 1 ℓ + 2 τ_{had} $t\bar{t}H$ multilepton 2 opposite-sign ℓ + 1 τ_{had} $t\bar{t}H$ multilepton 2 same-sign ℓ (categories for 0 or 1 τ_{had}) $t\bar{t}H$ multilepton 3 ℓ (categories for 0 or 1 τ_{had}) $t\bar{t}H$ multilepton 4 ℓ (except $H\to ZZ^*\to 4\ell$) $t\bar{t}H$ leptonic, $H\to ZZ^*\to 4\ell$ $t\bar{t}H$ hadronic, $H\to ZZ^*\to 4\ell$			$t\bar{t}H$ 1 ℓ, boosted $t\bar{t}H$ 1 ℓ, resolved (11 categories) $t\bar{t}H$ 2 ℓ (7 categories)
VH	VH 2 ℓ VH 1 ℓ, $p_{\mathrm{T}}^{\ell+E_{\mathrm{T}}^{\mathrm{miss}}}$ ≥ 150 GeV VH 1 ℓ, $p_{\mathrm{T}}^{\ell+E_{\mathrm{T}}^{\mathrm{miss}}}$ <150 GeV VH $E_{\mathrm{T}}^{\mathrm{miss}}$, $E_{\mathrm{T}}^{\mathrm{miss}}$ ≥ 150 GeV VH $E_{\mathrm{T}}^{\mathrm{miss}}$, $E_{\mathrm{T}}^{\mathrm{miss}}$ <150 GeV VH+VBF p_{T}^{j1} ≥ 200 GeV VH hadronic (2 categories)	VH leptonic 0-jet, $p_{\mathrm{T}}^{4\ell} \geq 100$ GeV 2-jet, $m_{jj} < 120$ GeV			2 ℓ, $75 \leq p_{\mathrm{T}}^{V} < 150$ GeV, $N_{\mathrm{jets}} = 2$ 2 ℓ, $75 \leq p_{\mathrm{T}}^{V} < 150$ GeV, $N_{\mathrm{jets}} \geq 3$ 2 ℓ, $p_{\mathrm{T}}^{V} \geq 150$ GeV, $N_{\mathrm{jets}} = 2$ 2 ℓ, $p_{\mathrm{T}}^{V} \geq 150$ GeV, $N_{\mathrm{jets}} \geq 3$ 1 ℓ $p_{\mathrm{T}}^{V} \geq 150$ GeV, $N_{\mathrm{jets}} = 2$ 1 ℓ $p_{\mathrm{T}}^{V} \geq 150$ GeV, $N_{\mathrm{jets}} = 3$ 0 ℓ, $p_{\mathrm{T}}^{V} \geq 150$ GeV, $N_{\mathrm{jets}} = 2$ 0 ℓ, $p_{\mathrm{T}}^{V} \geq 150$ GeV, $N_{\mathrm{jets}} = 3$
VBF	VBF, $p_{\mathrm{T}}^{\gamma\gamma jj}$ ≥ 25 GeV (2 categories) VBF, $p_{\mathrm{T}}^{\gamma\gamma jj}$<25 GeV (2 categories)	2-jet VBF, $p_{\mathrm{T}}^{j1} \geq 200$ GeV 2-jet VBF, p_{T}^{j1}<200 GeV	2-jet VBF	VBF $p_{\mathrm{T}}^{\tau\tau} > 140$ GeV ($\tau_{\mathrm{had}}\tau_{\mathrm{had}}$ only) VBF high-m_{jj} VBF low-m_{jj}	VBF, two central jets VBF, four central jets VBF +γ
ggF	2-jet, $p_{\mathrm{T}}^{\gamma\gamma}$ ≥ 200 GeV 2-jet, 120 GeV ≤ $p_{\mathrm{T}}^{\gamma\gamma}$¡200 GeV 2-jet, 60 GeV ≤ $p_{\mathrm{T}}^{\gamma\gamma}$¡120 GeV 2-jet, $p_{\mathrm{T}}^{\gamma\gamma}$ < 60 GeV 1-jet, $p_{\mathrm{T}}^{\gamma\gamma}$ ≥ 200 GeV 1-jet, 120 GeV ≤ $p_{\mathrm{T}}^{\gamma\gamma}$¡200 GeV 1-jet, 60 GeV ≤ $p_{\mathrm{T}}^{\gamma\gamma}$¡120 GeV 1-jet, $p_{\mathrm{T}}^{\gamma\gamma}$ < 60 GeV 0-jet (2 categories)	1-jet, $p_{\mathrm{T}}^{4\ell} \geq 120$ GeV 1-jet, 60 GeV≤ $p_{\mathrm{T}}^{4\ell}$¡120 GeV 1-jet, $p_{\mathrm{T}}^{4\ell} < 60$ GeV 0-jet, $p_{\mathrm{T}}^{4\ell} < 100$ GeV	1-jet, $m_{\ell\ell} < 30$ GeV, $p_{\mathrm{T}}^{\ell_2} < 20$ GeV 1-jet, $m_{\ell\ell} < 30$ GeV, $p_{\mathrm{T}}^{\ell_2} \geq 20$ GeV 1-jet, $m_{\ell\ell} \geq 30$ GeV, $p_{\mathrm{T}}^{\ell_2} < 20$ GeV 1-jet, $m_{\ell\ell} \geq 30$ GeV, $p_{\mathrm{T}}^{\ell_2} \geq 20$ GeV 0-jet, $m_{\ell\ell} < 30$ GeV, $p_{\mathrm{T}}^{\ell_2} < 20$ GeV 0-jet, $m_{\ell\ell} < 30$ GeV, $p_{\mathrm{T}}^{\ell_2} \geq 20$ GeV 0-jet, $m_{\ell\ell} \geq 30$ GeV, $p_{\mathrm{T}}^{\ell_2} < 20$ GeV 0-jet, $m_{\ell\ell} \geq 30$ GeV, $p_{\mathrm{T}}^{\ell_2} \geq 20$ GeV	Boosted, $p_{\mathrm{T}}^{\tau\tau} > 140$ GeV Boosted, $p_{\mathrm{T}}^{\tau\tau} \leq 140$ GeV	

$$\mu = 1.11^{+0.09}_{-0.08} = 1.11 \pm 0.05\,(\mathrm{stat.})\,^{+0.05}_{-0.04}\,(\mathrm{exp.})\,^{+0.05}_{-0.04}\,(\mathrm{sig.\ th.})\,^{+0.03}_{-0.03}\,(\mathrm{bkg.\ th.})$$

Higgs Production Modes

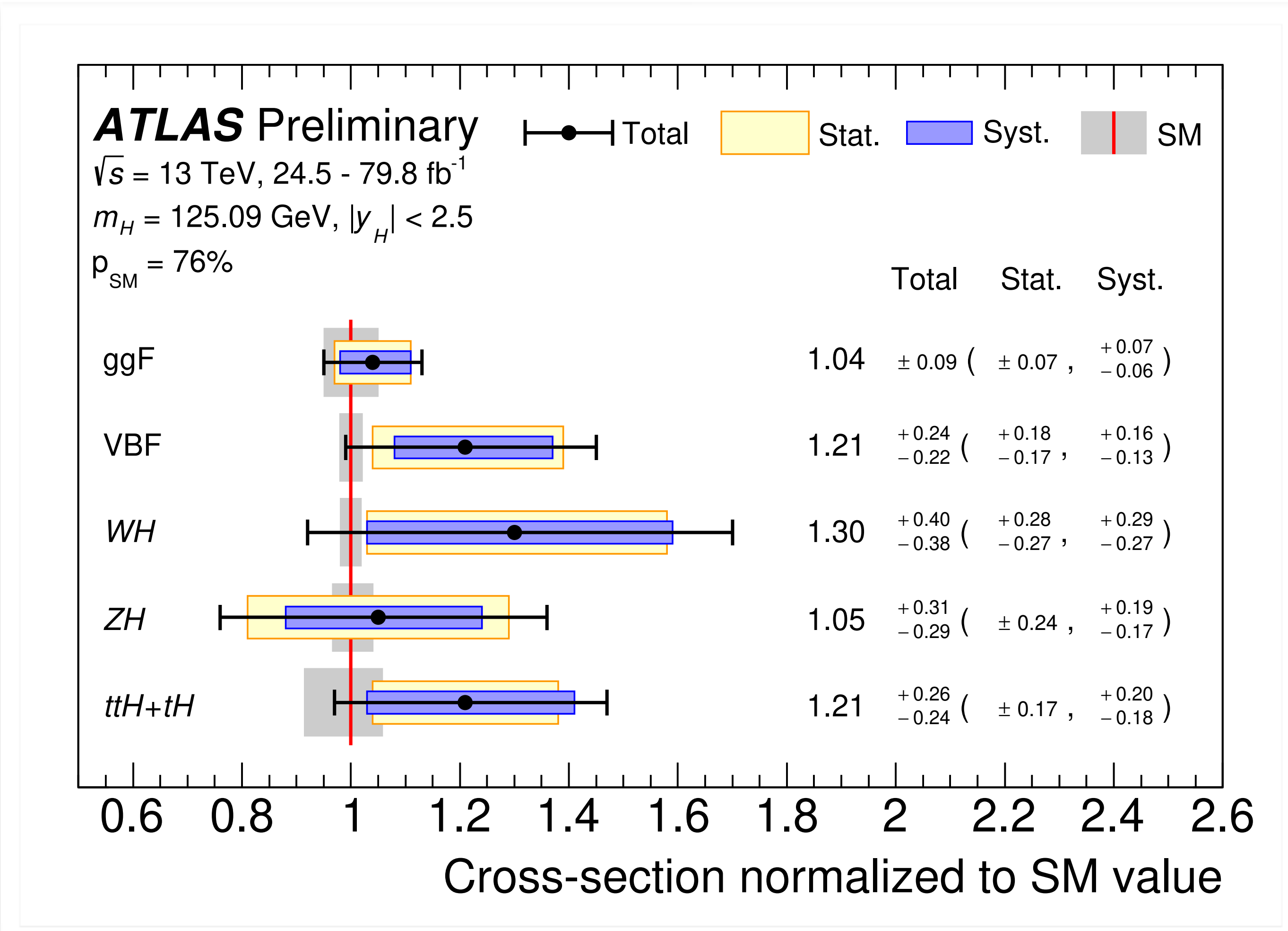

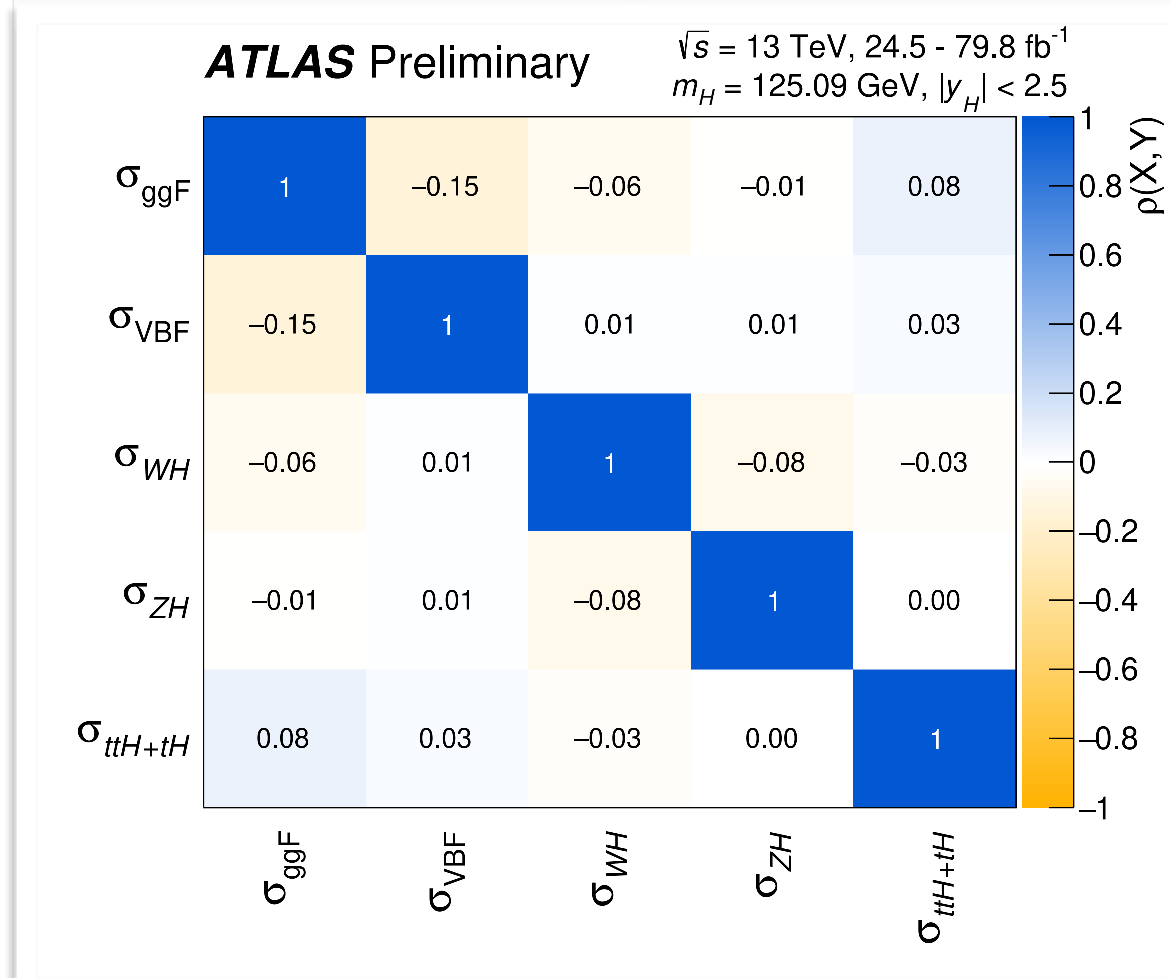

- Significances above 5σ are obtained for ggF, VBF (6.5σ), VH (5.3σ) and ttH (5.8σ) production modes when assuming SM branching ratios
- Low correlations between production modes
- Results are consistent with predictions from the Standard Model

ATLAS-CONF-2019-005

Production and Decay Modes

NEW

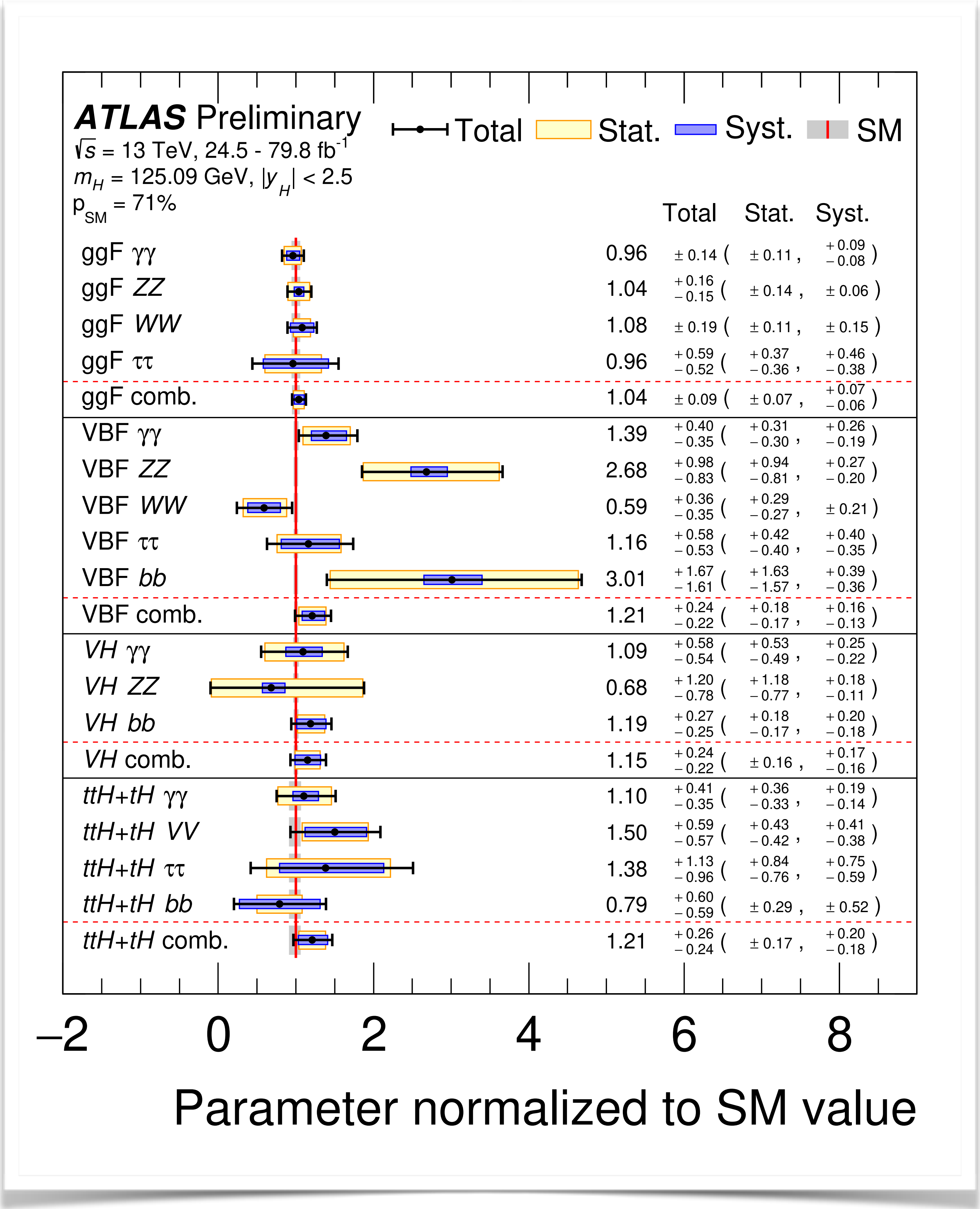

Fix production/decays with low sensitivity to SM values

ATLAS-CONF-2019-005

Coupling vs Mass

NEW

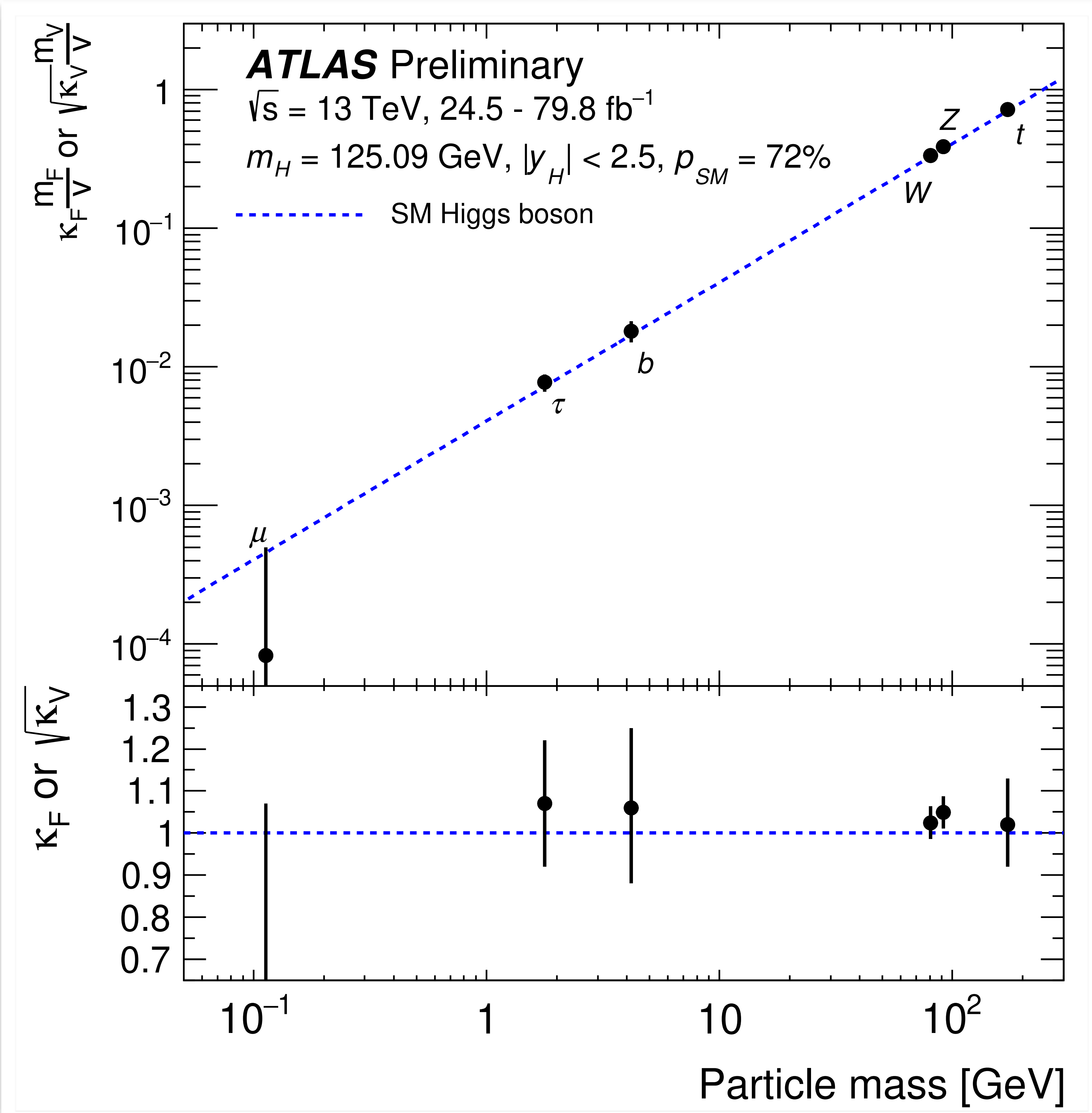

Interpret the results in the κ framework as a function of the particle mass assuming no BSM contributions to the total width

$$\kappa_j^2 = \frac{\sigma_j}{\sigma_j^{\mathrm{SM}}} \quad \text{or} \quad \kappa_j^2 = \frac{\Gamma^j}{\Gamma^j_{\mathrm{SM}}}$$

ATLAS-CONF-2019-005

Probing BSM Contributions

Explore three different scenarios for the total width

All scale factors measured to be compatible with SM expectations

- If $|\kappa_V| < 1$;
  - $B_{inv} < 0.30$ (0.18) and
  - $B_{undet} < 0.22$ (0.38)
- Off-shell $H \rightarrow ZZ \rightarrow 4l$ measurement
  - if $\kappa_{on} = \kappa_{off}$;
    - $B_{BSM} < 0.47$ (0.57)

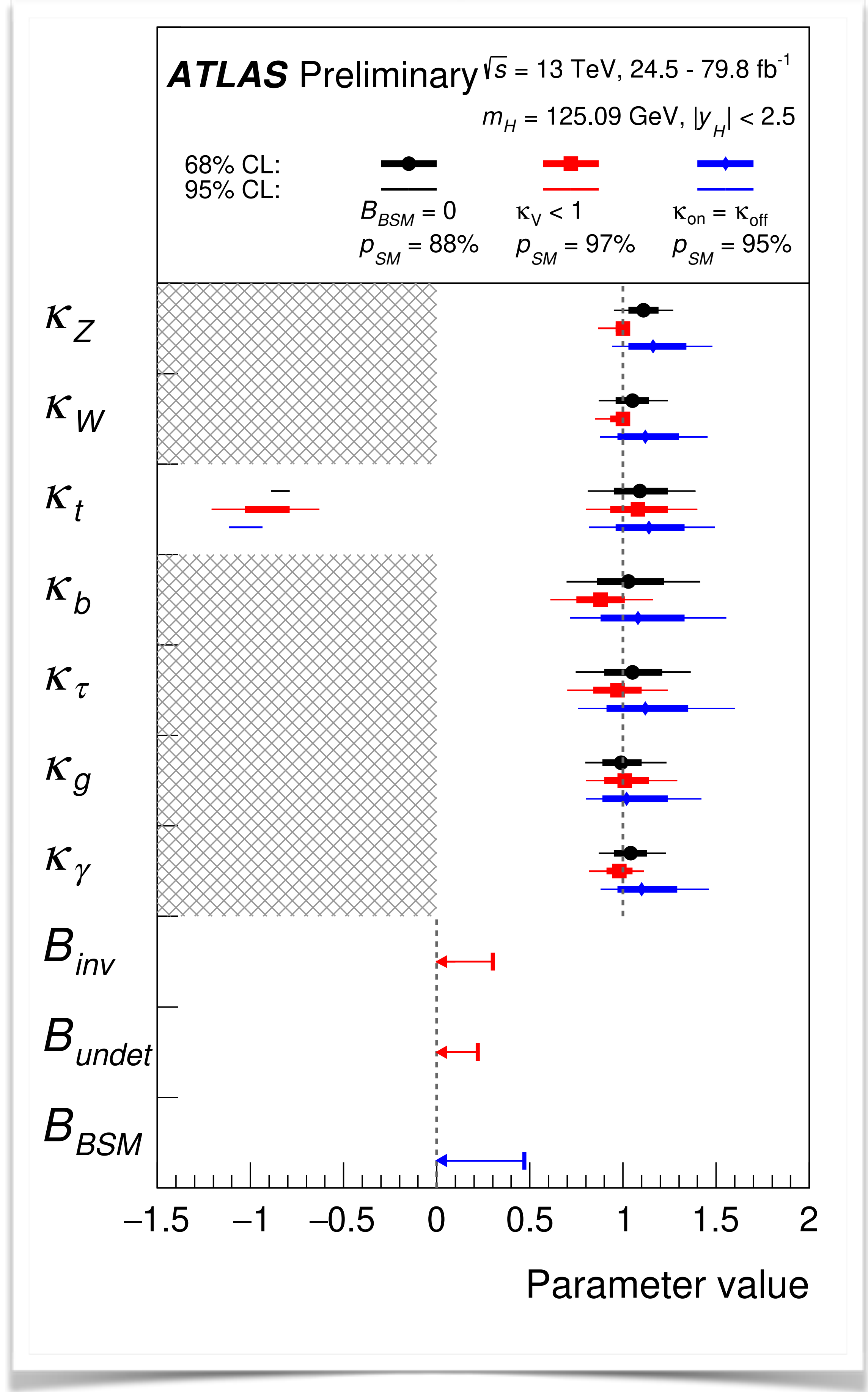

NEW

ATLAS-CONF-2019-005

Probing the Higgs Self-coupling

NEW

- Starting from the Higgs potential

$$V(H) = \frac{1}{2}m_H^2 + \lambda_3 \nu H^3 + \frac{1}{4}\lambda_4 H^3 + O(H^5)$$

- Consider modifications: $\lambda_3 = \kappa_\lambda \lambda_3^{SM}$
- Modified Higgs production cross-sections:

$$\mu_i(\kappa_\lambda, \kappa_i) = \frac{\sigma^{\mathrm{BSM}}}{\sigma^{\mathrm{SM}}} = Z_H^{\mathrm{BSM}}(\kappa_\lambda)\left[\kappa_i^2 + \frac{(\kappa_\lambda - 1)C_1^i}{K_{\mathrm{EW}}^i}\right]$$

$$Z_H^{\mathrm{BSM}}(\kappa_\lambda) = \frac{1}{1-(\kappa_\lambda^2 - 1)\delta Z_H} \quad \text{with} \quad \delta Z_H = -1.536\times 10^{-3}$$

- Modified branching fractions

$$\mu_f(\kappa_\lambda, \kappa_f) = \frac{\mathrm{BR}_f^{\mathrm{BSM}}}{\mathrm{BR}_f^{SM}} = \frac{\kappa_f^2 + (\kappa_\lambda - 1)C_1^f}{\sum_j \mathrm{BR}_j^{\mathrm{SM}}\left[\kappa_j^2 + (\kappa_\lambda - 1)C_1^j\right]}$$

- Apply fit to Higgs combination (incl. STXS):

$$\kappa_\lambda = 4.0^{+3.7}_{-3.6}(\mathrm{stat.})^{+1.6}_{-1.5}(\mathrm{exp.})^{+1.3}_{-0.9}(\mathrm{sig.th})^{+0.8}_{-0.9}(\mathrm{bkg.th})$$

$-3.2 < \kappa_\lambda < 11.9$ @ 95% CL

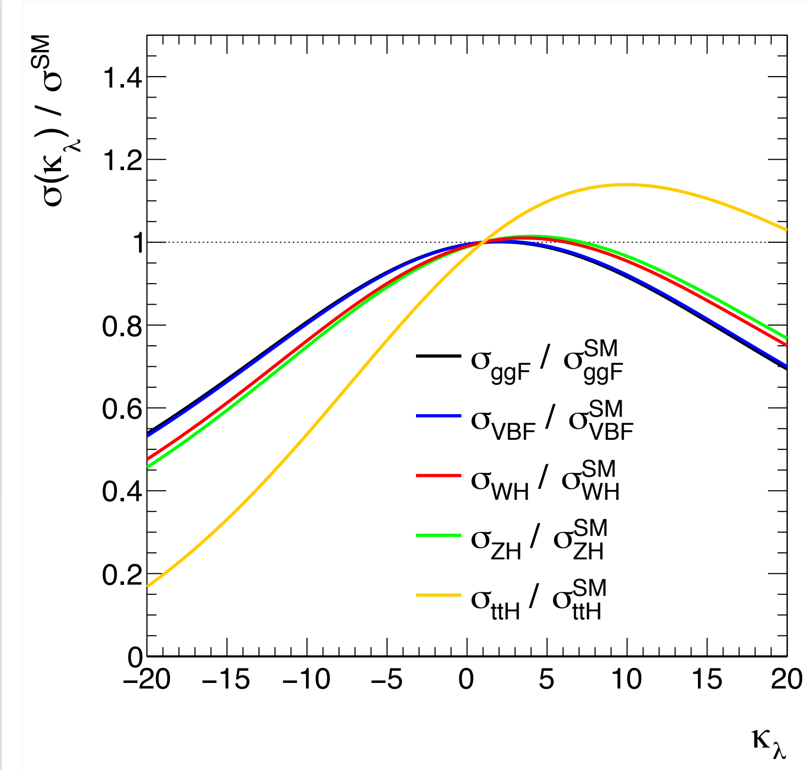

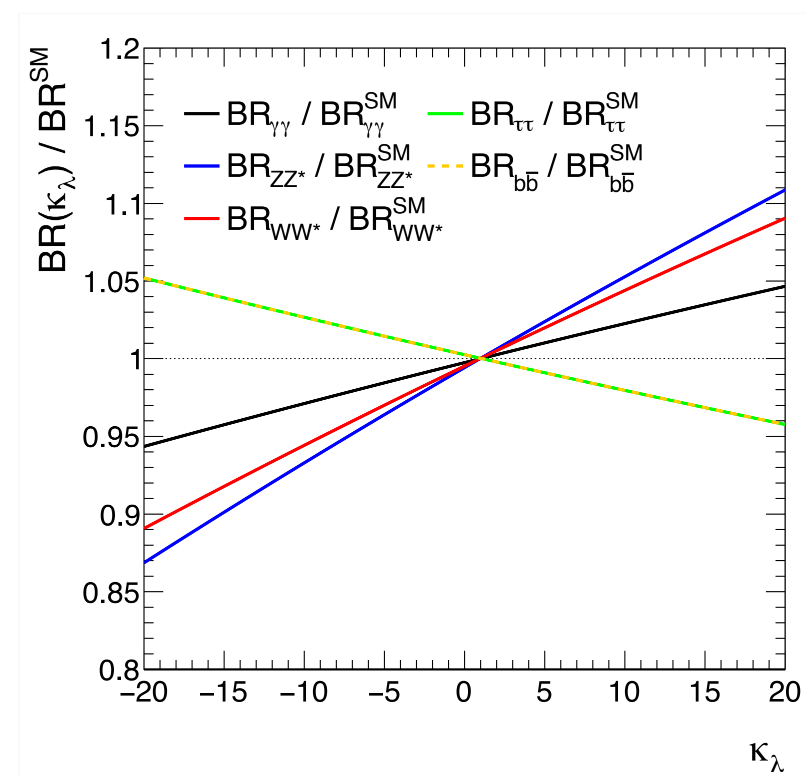

JHEP12 (2016) 080, EPJC 77 (2017) 887, ATL-PHYS-PUB-2019-009

Conclusion

- Highlights since Moriond last year include
  - Observation of the coupling of the **Higgs to bottom quarks**
  - Observation of the coupling of the **Higgs to top quarks**
  - **New combination** with observation of **all main LHC Higgs production modes**
- So far, the results seem to agree to a remarkable degree to the Standard Model predictions…
  - But more data and more results to come

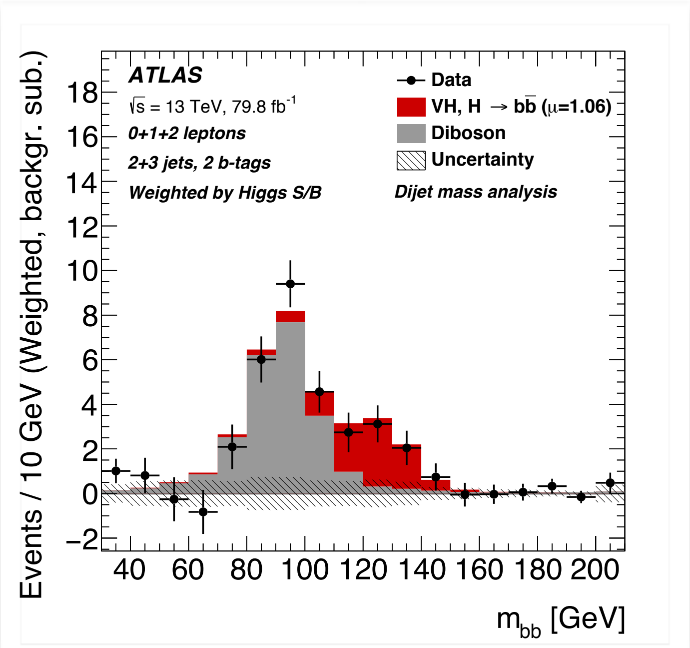

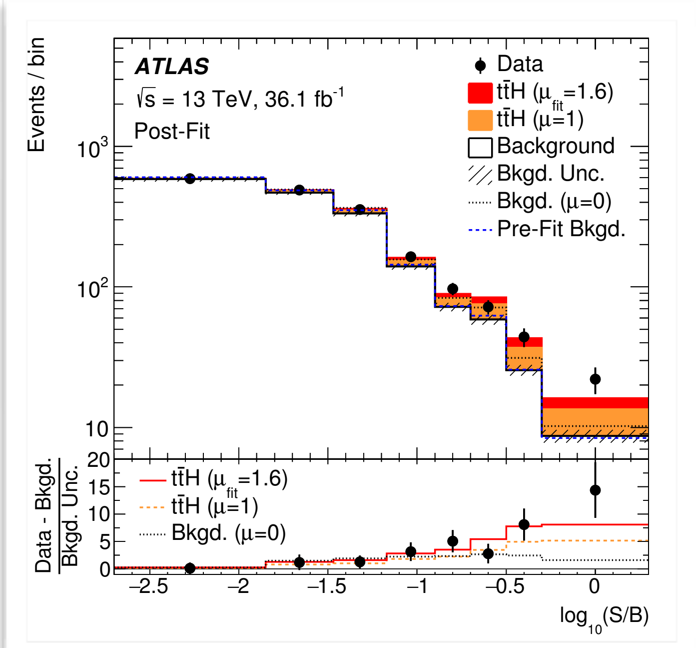

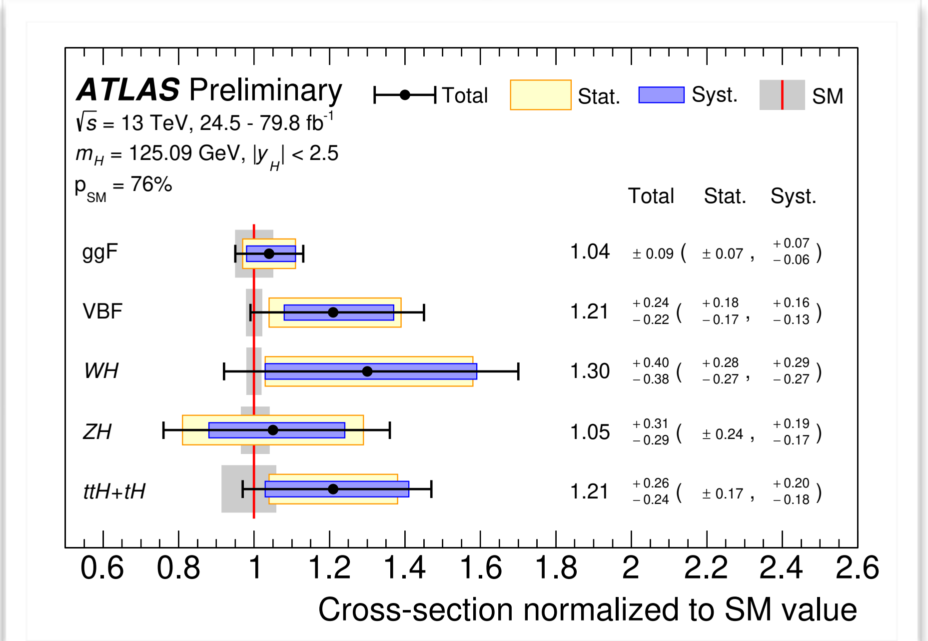

See talks by F. Cerutti, H. Wang and J. Dickinson for more details

Backup

κ_λ

ATL-PHYS-PUB-2019-009

Feynman Diagrams for κλ

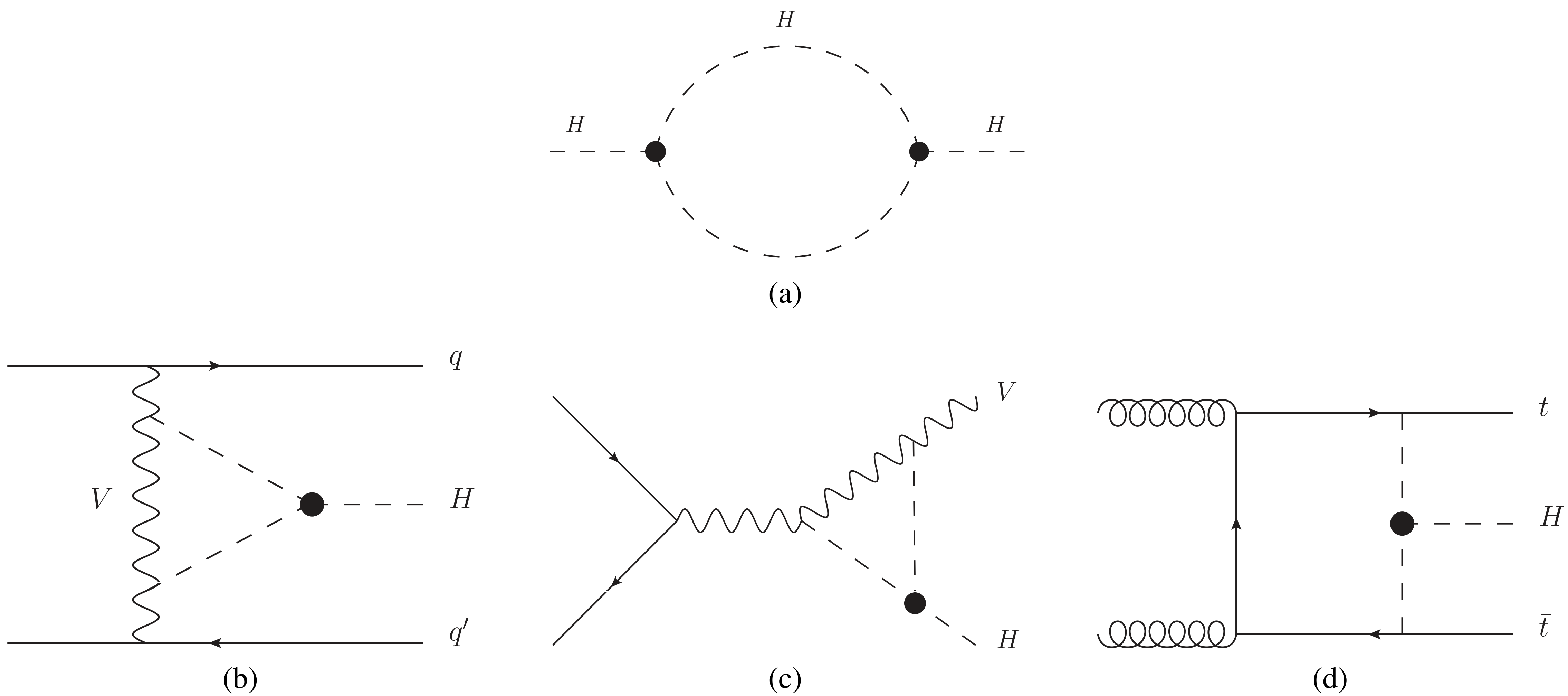

Figure 1: Examples of one loop λ_{HHH}-dependent diagrams for the Higgs boson self energy (a) and the single Higgs boson production in the VBF (b), VH (c), and $t\bar{t}H$ (d) modes. The self-coupling vertex is indicated by the filled circle.

Categories used for κλ

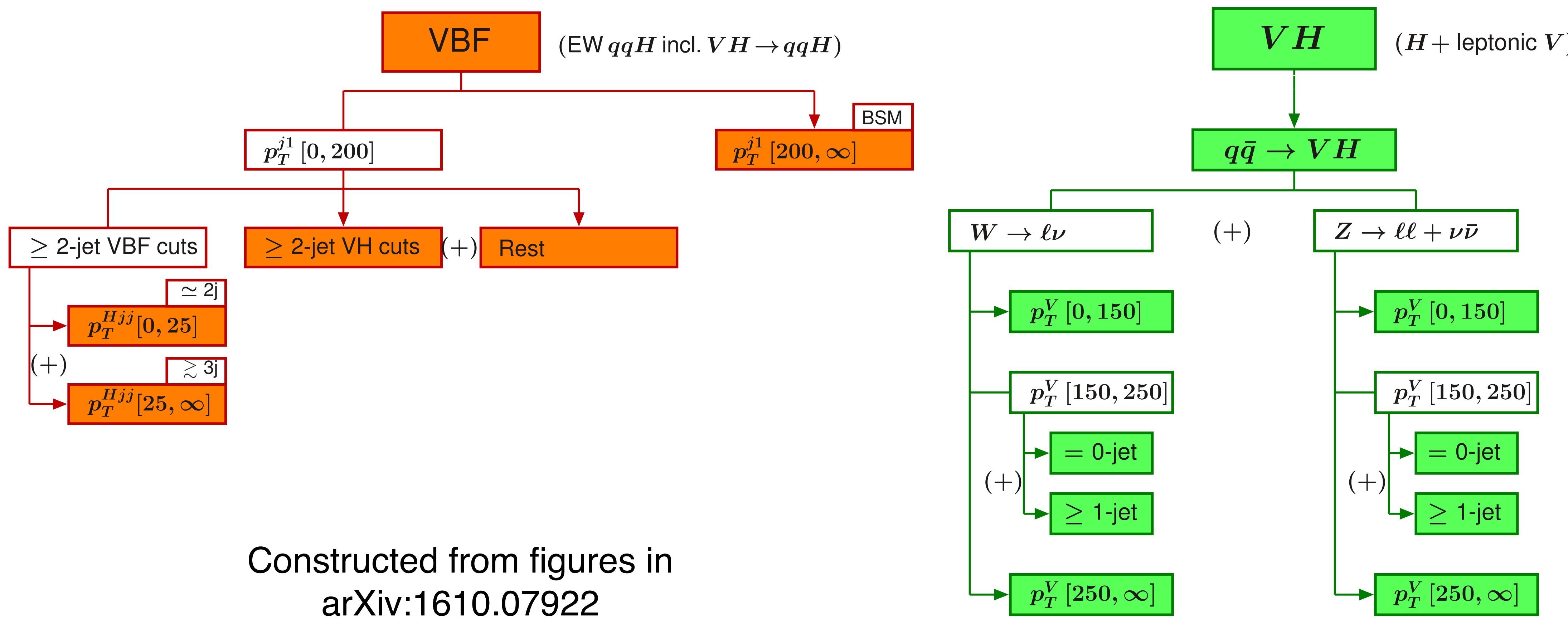

Figure 3: Schematic diagram of the VBF + V(had)H (left) and V(lep)H (right) STXS regions. p_{T}^{Hjj} is the p_{T} of the Higgs boson plus two jets system, p_{T}^{V} is the p_{T} of the vector boson V in the VH production mode, p_{T}^{j1} is the p_{T} of the jet with the highest p_{T}. In the VH, $H \to b\bar{b}$ analysis, the separation in jet number of the p_{T}^{V} [150, 250] region in the VH production mode has been ignored, merging the 0 and the ≥ 1 jet regions. The diagrams are obtained from Ref. [14].

Categories used for κλ

STXS bin		VBF	WH	ZH
		$C_1^i \times 100$		
VBF + V(had)H	VBF-cuts + $p_T^{j1} < 200$ GeV, $\leq 2j$	0.63	0.91	1.07
	VBF-cuts + $p_T^{j1} < 200$ GeV, $\geq 3j$	0.61	0.85	1.04
	VH-cuts + $p_T^{j1} < 200$ GeV	0.64	0.89	1.10
	no VBF/VH-cuts, $p_T^{j1} < 200$ GeV	0.65	1.13	1.28
	$p_T^{j1} > 200$ GeV	0.39	0.23	0.28
$qq \to H\ell\nu$	$p_T^V < 150$ GeV		1.15	
	$150 < p_T^V < 250$ GeV, $0j$		0.18	
	$150 < p_T^V < 250$ GeV, $\geq 1j$		0.33	
	$p_T^V > 250$ GeV		0	
$qq \to H\ell\ell$ $qq \to H\nu\nu$	$p_T^V < 150$ GeV			1.33
	$150 < p_T^V < 250$ GeV, $0j$			0.20
	$150 < p_T^V < 250$ GeV, $\geq 1j$			0.39
	$p_T^V > 250$ GeV			0

Table 5: C_1^i coefficients for each region of the STXS scheme for the VBF, WH and ZH production modes. The same definition for STXS regions and production modes as in Table 2 is used. In the VBF categories, "VBF-cuts" [14] indicates selections applied to target the VBF di-jet topology, with requirements on the di-jet invariant mass (m_{jj}) and the difference in pseudorapidity between the two jets; the additional $\leq 2j$ and $\geq 3j$ bin separation is performed indirectly by requesting $p_T^{Hjj} \lessgtr 25$ GeV. "VH-cuts" select the $W, Z \to jj$ decays, requiring an m_{jj} value close to the vector boson mass [14]. The C_1^i coefficients of the $p_T^V > 250$ GeV regions are negligible, O(10^{-6}), and are set to 0.

H vs HH

- H
  - $\kappa_\lambda = 4.0^{+3.7}_{-3.6}(\mathrm{stat.})^{+1.6}_{-1.5}(\mathrm{exp.})^{+1.3}_{-0.9}(\mathrm{sig.th})^{+0.8}_{-0.9}(\mathrm{bkg.th})$
  - Observed: $-3.2 < \kappa_\lambda < 11.9$ @ 95% CL
  - Expected: $-6.2 < \kappa_\lambda < 14.4$ @ 95% CL

~80 fb^{-1}

- HH
  - Observed: $-5.0 < \kappa_\lambda < 12.1$ @ 95% CL
  - Expected: $-5.8 < \kappa_\lambda < 12.0$ @ 95% CL

~36 fb^{-1}

Likelihoods

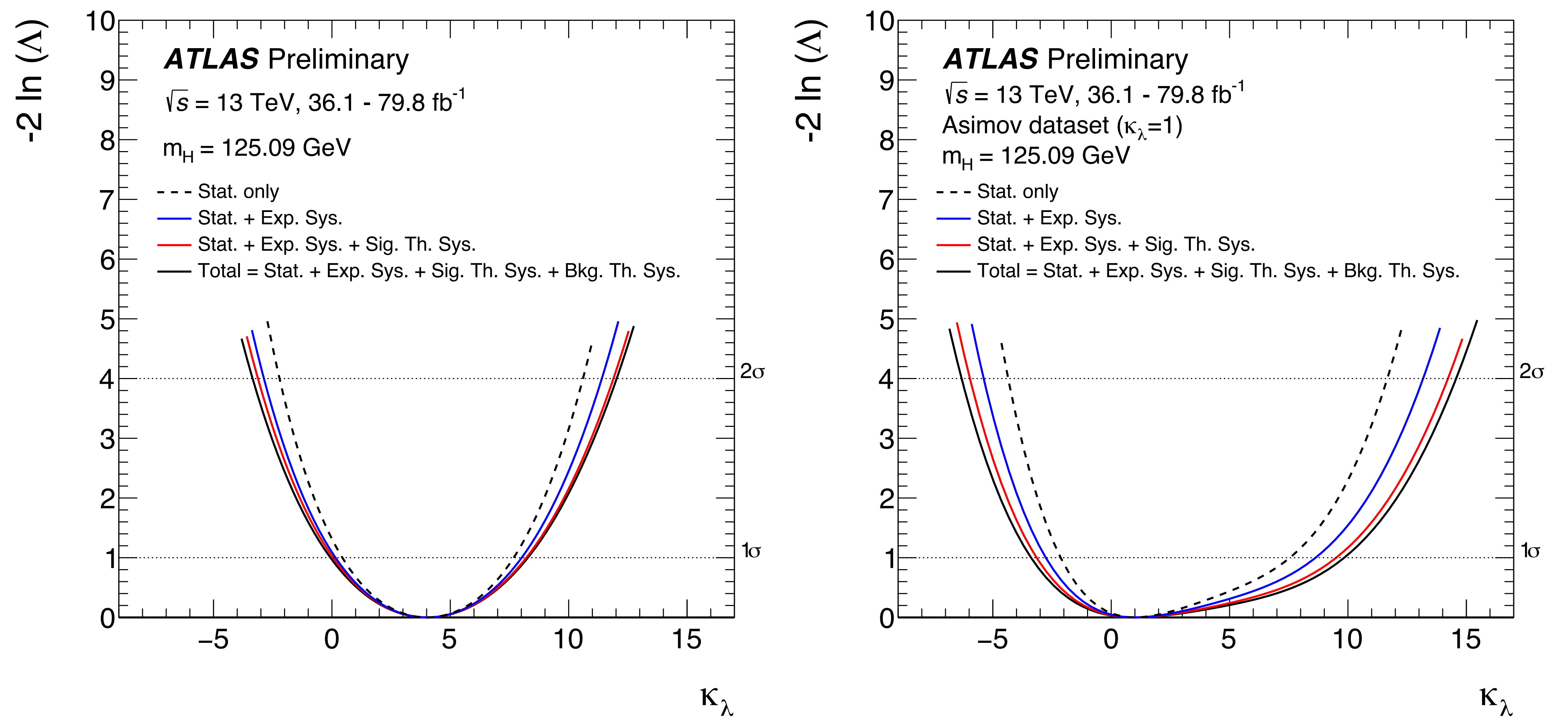

(a) (b)

Figure 4: Profile likelihood scan, in terms of $-2\ln\Lambda(\kappa_\lambda)$, performed as a function of κ_λ on data (a) and on the Asimov dataset [32] generated under the SM hypothesis (b). The solid black line shows the profile likelihood distributions obtained including all systematic uncertainties ("Total"). Results from a statistic only fit "Stat. only" (black dashed line), including the experimental systematics "Stat. + Exp. Sys." (blue solid line) , adding theory systematics related to the signal "Stat.+ Exp. Sys.+ Sig. Th. Sys." (red solid line) are also shown. The dotted horizontal lines show the $-2\ln\Lambda(\kappa_\lambda) = 1$ and $-2\ln\Lambda(\kappa_\lambda) = 4$ levels that are used to define the $\pm1\sigma$ and $\pm2\sigma$ uncertainties on κ_λ.

Likelihoods by Channel

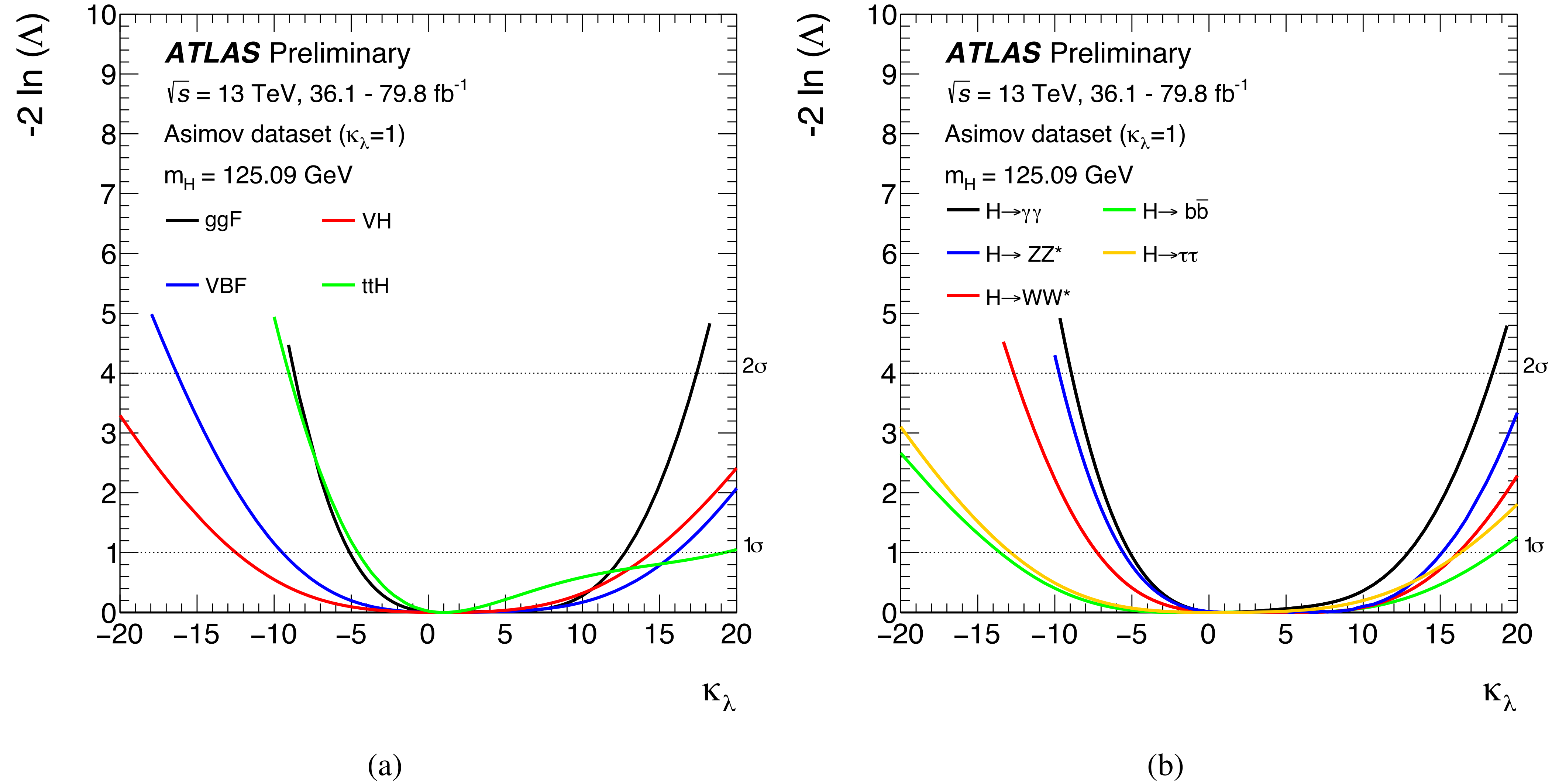

Figure 5: Profile likelihood scan, in terms of $-2\ln\Lambda(\kappa_\lambda)$, performed as a function of κ_λ on Asimov datasets [32] generated under the SM hypothesis for each Higgs boson production mode (a) and each decay channel (b). In (a) the scan is performed parametrising all branching fractions and the selected production mode cross section as a function of κ_λ, while freely floating the signal strengths of the other production modes, in (b) all production mode cross sections and decay branching fractions are expressed as a function of κ_λ, but only the categories of the selected channel are included in the fit. The $t\bar{t}H$ multi-lepton categories are excluded from the $H \to ZZ^*$, $H \to WW^*$, and $H \to \tau\tau$ fits.

Likelihood Contours

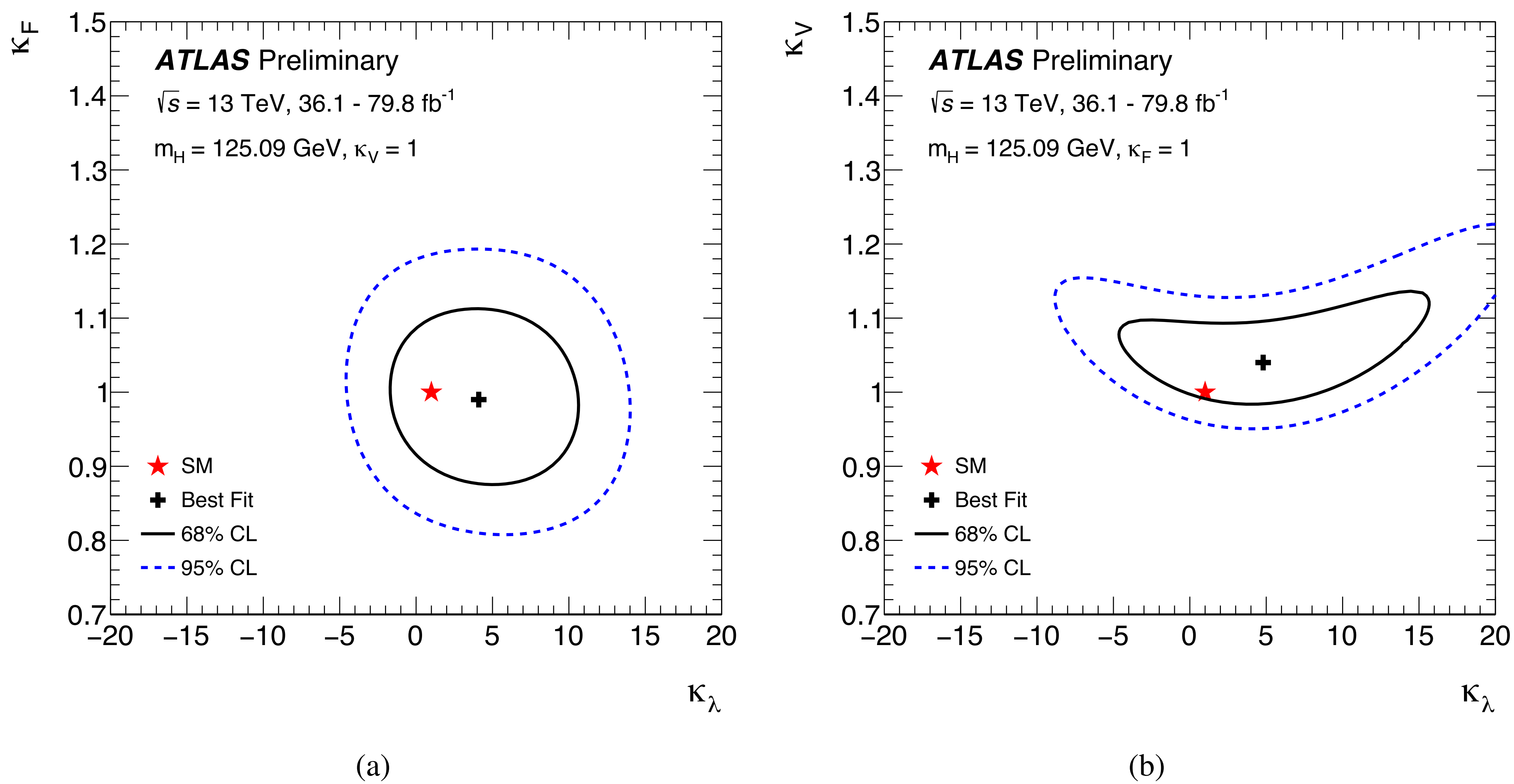

Figure 6: Negative log-likelihood contours at 68% and 95% C.L. in the $(\kappa_\lambda, \kappa_F)$ plane under the assumption of $\kappa_V = 1$ (a), and in the $(\kappa_\lambda, \kappa_V)$ plane under the assumption of $\kappa_F = 1$ (b). The best fit value is indicated by a cross while the SM hypothesis is indicated by a star. The plot assumes that the approximations in Refs. [8,9] are valid inside the shown contours.

κ from different fits

POIs	Granularity	$\kappa_F{}^{+1\sigma}_{-1\sigma}$	$\kappa_V{}^{+1\sigma}_{-1\sigma}$	$\kappa_\lambda{}^{+1\sigma}_{-1\sigma}$	κ_λ [95% C.L.]
κ_λ	STXS	1	1	$4.0^{+4.3}_{-4.1}$	$[-3.2, 11.9]$
				$1.0^{+8.8}_{-4.4}$	$[-6.2, 14.4]$
κ_λ	inclusive	1	1	$4.6^{+4.3}_{-4.2}$	$[-2.9, 12.5]$
				$1.0^{+9.5}_{-4.3}$	$[-6.1, 15.0]$
κ_λ, κ_V	STXS	1	$1.04^{+0.05}_{-0.04}$	$4.8^{+7.4}_{-6.7}$	$[-6.7, 18.4]$
			$1.00^{+0.05}_{-0.04}$	$1.0^{+9.9}_{-6.1}$	$[-9.4, 18.9]$
κ_λ, κ_F	STXS	$0.99^{+0.08}_{-0.08}$	1	$4.1^{+4.3}_{-4.1}$	$[-3.2, 11.9]$
		$1.0^{+0.08}_{-0.08}$		$1.0^{+8.8}_{-4.4}$	$[-6.3, 14.4]$

Table 6: Best fit values for κ modifiers with $\pm 1\sigma$ uncertainties. The first column shows the parameter(s) of interest in each fit configuration, where the other coupling modifiers are kept fixed to the SM prediction. The fit to determine κ_λ has been performed in two configurations, one using the full STXS granularity for VBF, ZH and WH (STXS), and the other only considering the inclusive parametrization for all the production modes (inclusive). The 95% C.L. interval for κ_λ is also reported. For each fit result the upper row corresponds to the observed results, and the lower row to the expected results obtained using Asimov datasets generated under the SM hypothesis [32]. The κ_λ, κ_V and κ_λ, κ_F fit results are obtained under the assumption that the approximations in Refs. [8,9] are valid in 95% C.L. regions.

Combination

ATLAS-CONF-2019-005

Luminosity in Combination

Table 1: Integrated luminosity of the dataset used for each input analysis to the combination.

Analysis	Integrated luminosity (fb^{-1})
$H \to \gamma\gamma$ (including $t\bar{t}H$, $H \to \gamma\gamma$)	79.8
$H \to ZZ^* \to 4\ell$ (including $t\bar{t}H$, $H \to ZZ^* \to 4\ell$)	79.8
$H \to WW^* \to e\nu\mu\nu$	36.1
$H \to \tau\tau$	36.1
VH, $H \to b\bar{b}$	79.8
VBF, $H \to b\bar{b}$	24.5 – 30.6
$H \to \mu\mu$	79.8
$t\bar{t}H$, $H \to b\bar{b}$ and $t\bar{t}H$ multilepton	36.1
$H \to$ invisible	36.1
Off-shell $H \to ZZ^* \to 4\ell$ and $H \to ZZ^* \to 2\ell2\nu$	36.1

Likelihood in the Combination

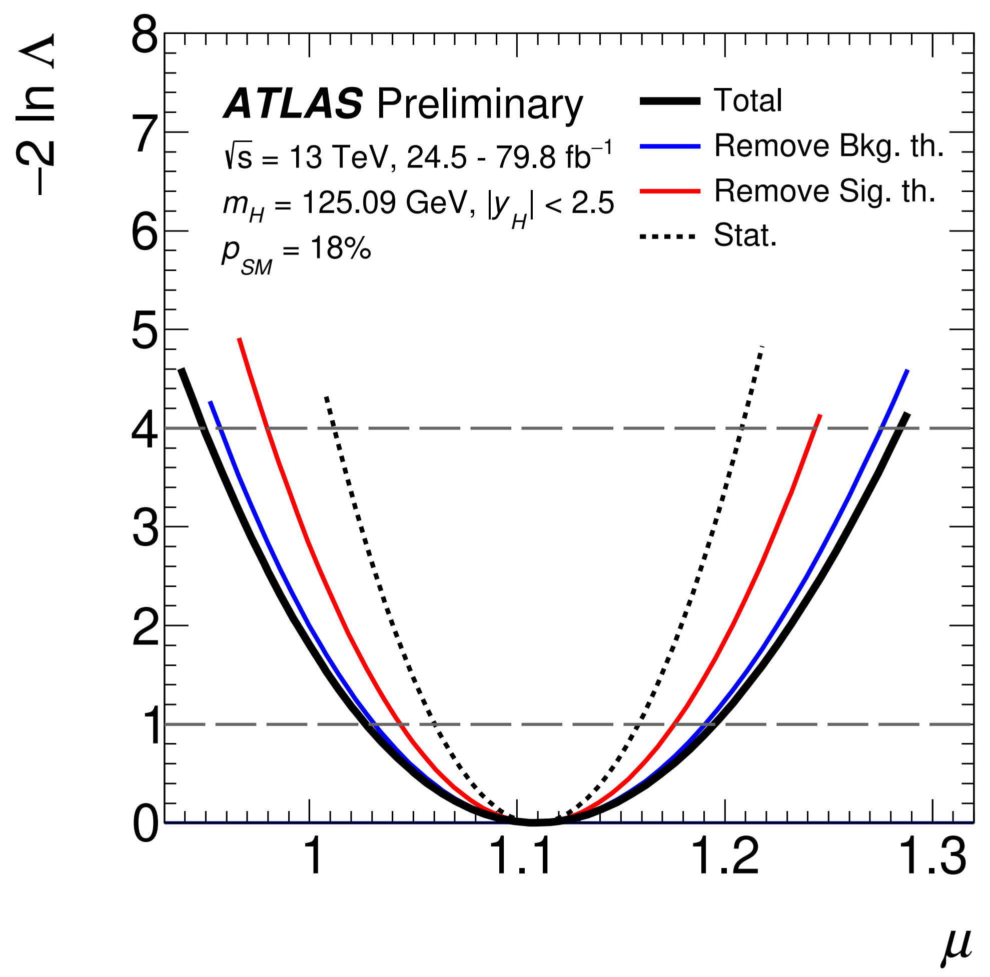

Figure 1: Variations of $-2\ln\Lambda(\mu)$ as a function of μ with all systematic uncertainties included (solid black line), with parameters describing theory uncertainties on background processes fixed to their best-fit values (solid blue line), with the same procedure also applied to theory uncertainties on the signal process (solid red line) and all systematic uncertainties (dotted black line). The dashed horizontal lines show the levels $-2\ln\Lambda(\mu) = 1$ and $-2\ln\Lambda(\mu) = 4$ which are used to define, respectively, the 1σ and 2σ confidence intervals on μ, as described in Section 4.

Combination Systematics

Table 3: Summary of the relative uncertainties $\Delta\mu/\mu$ affecting the measurement of the combined global signal strength μ. "MC stat." refers to uncertainties due to limited numbers of simulated events. "Other" refers to the combined effect of the sources of experimental systematic uncertainty not explicitly listed in the table.

Uncertainty source	$\Delta\mu/\mu$ [%]
Statistical uncertainty	4.4
Systematic uncertainties	6.2
Theory uncertainties	4.8
Signal	4.2
Background	2.6
Experimental uncertainties (excl. MC stat.)	4.1
Luminosity	2.0
Background modeling	1.6
Jets, $E_{\mathrm{T}}^{\mathrm{miss}}$	1.4
Flavour tagging	1.1
Electrons, photons	2.2
Muons	0.2
τ-lepton	0.4
Other	1.6
MC statistical uncertainty	1.7
Total uncertainty	7.6

Breakdown for Combination Cross-sections

Table 4: Best-fit values and uncertainties of the production cross sections of the Higgs boson, assuming SM values for its decay branching fractions. The total uncertainties are decomposed into components for data statistics (Stat.), experimental systematic uncertainties (Exp.), and theory uncertainties in the modeling of the signal (Sig. th.) and background (Bkg. th.) processes. SM predictions [26] are shown for the cross section of each production process. The observed (obs.) and expected (exp.) significances of the observed signals relative to the no-signal hypothesis are also shown for all processes except ggF, which was observed in Run 1. For the WH and ZH modes, a combined VH significance is reported assuming the SM value of the ratio of WH to ZH production.

Process ($\|y_H\| < 2.5$)	Value [pb]	Uncertainty [pb] Total	Stat.	Exp.	Sig. th.	Bkg. th.	SM pred. [pb]	Significance obs. (exp.)	
ggF	46.5	±4.0	±3.1	±2.2	±0.9	±1.3	44.7 ± 2.2	-	
VBF	4.25	$^{+0.84}_{-0.77}$	$^{+0.63}_{-0.60}$	$^{+0.35}_{-0.32}$	$^{+0.42}_{-0.32}$	$^{+0.14}_{-0.11}$	3.515 ± 0.075	6.5 (5.3)	
WH	1.57	$^{+0.48}_{-0.46}$	$^{+0.34}_{-0.33}$	$^{+0.25}_{-0.24}$	$^{+0.11}_{-0.07}$	±0.20	1.204 ± 0.024	3.5 (2.7)	5.3 (4.7)
ZH	0.84	$^{+0.25}_{-0.23}$	±0.19	±0.09	$^{+0.07}_{-0.04}$	±0.10	$0.797^{+0.033}_{-0.026}$	3.6 (3.6)	
$t\bar{t}H+tH$	0.71	$^{+0.15}_{-0.14}$	±0.10	±0.07	$^{+0.05}_{-0.04}$	$^{+0.08}_{-0.07}$	$0.586^{+0.034}_{-0.049}$	5.8 (5.4)	

Systematics Breakdown for Combination

Table 5: Summary of the uncertainties affecting the production cross section measurements. "MC stat." refers to uncertainties due to limited numbers of simulated events. "Other" refers to the combined effect of the sources of experimental systematic uncertainty not explicitly listed in the table.

Uncertainty source	$\frac{\Delta\sigma_{ggF}}{\sigma_{ggF}}$ [%]	$\frac{\Delta\sigma_{VBF}}{\sigma_{VBF}}$ [%]	$\frac{\Delta\sigma_{WH}}{\sigma_{WH}}$ [%]	$\frac{\Delta\sigma_{ZH}}{\sigma_{ZH}}$ [%]	$\frac{\Delta\sigma_{t\bar{t}H+tH}}{\sigma_{t\bar{t}H+tH}}$ [%]
Statistical uncertainties	6.4	15	21	23	14
Systematic uncertainties	6.2	12	22	17	15
Theory uncertainties	3.4	9.2	14	14	12
Signal	2.0	8.7	5.8	6.7	6.3
Background	2.7	3.0	13	12	10
Experimental uncertainties (excl. MC stat.)	5.0	6.5	9.9	9.6	9.2
Luminosity	2.1	1.8	1.8	1.8	3.1
Background modeling	2.5	2.2	4.7	2.9	5.7
Jets, E_T^{miss}	0.9	5.4	3.0	3.3	4.0
Flavour tagging	0.9	1.3	7.9	8.0	1.8
Electrons, photons	2.5	1.7	1.8	1.5	3.8
Muons	0.4	0.3	0.1	0.2	0.5
τ-lepton	0.2	1.3	0.3	0.1	2.4
Other	2.5	1.2	0.3	1.1	0.8
MC statistical uncertainties	1.6	4.8	8.8	7.9	4.4
Total uncertainties	8.9	19	30	29	21

Systematics Breakdown for Combination (2)

Table 6: Best-fit values and uncertainties of the production cross sections times branching ratios of the Higgs boson, for the combinations in which sufficient sensitivity is provided by the input analyses. Combinations not shown in the table are fixed to their SM values within uncertainties. For $t\bar{t}H$+tH production, $H \to VV^*$ refers to the combination of $H \to WW^*$ and $H \to ZZ^*$, with a relative weight fixed by their respective SM branching fractions. The total uncertainties are decomposed into components for data statistics (Stat.), experimental systematic uncertainties (Exp.), and theory uncertainties in the modeling of the signal (Sig. th.) and background (Bkg. th.) processes. SM predictions [26] are shown for each process.

Process	Value	Uncertainty [fb]					SM pred.
($\|y_H\| < 2.5$)	[fb]	Total	Stat.	Exp.	Sig. th.	Bkg. th.	[fb]
ggF, $H \to \gamma\gamma$	97	±14	±11	±8	±2	$^{+2}_{-1}$	101.5 ± 5.3
ggF, $H \to ZZ^*$	1230	$^{+190}_{-180}$	±170	±60	±20	±20	1181 ± 61
ggF, $H \to WW^*$	10400	±1800	±1100	±1100	±380	$^{+960}_{-870}$	9600 ± 500
ggF, $H \to \tau\tau$	2700	$^{+1700}_{-1500}$	±1000	±920	$^{+810}_{-310}$	$^{+390}_{-420}$	2800 ± 140
VBF, $H \to \gamma\gamma$	11.1	$^{+3.2}_{-2.8}$	$^{+2.5}_{-2.4}$	$^{+1.4}_{-1.0}$	$^{+1.5}_{-1.1}$	$^{+0.3}_{-0.2}$	7.98 ± 0.21
VBF, $H \to ZZ^*$	249	$^{+91}_{-77}$	$^{+87}_{-75}$	$^{+16}_{-11}$	$^{+17}_{-12}$	$^{+9}_{-7}$	92.8 ± 2.3
VBF, $H \to WW^*$	450	$^{+270}_{-260}$	$^{+220}_{-200}$	$^{+120}_{-130}$	$^{+80}_{-70}$	$^{+70}_{-80}$	756 ± 19
VBF, $H \to \tau\tau$	260	$^{+130}_{-120}$	±90	$^{+80}_{-70}$	$^{+30}_{-10}$	$^{+30}_{-20}$	220 ± 6
VBF, $H \to b\bar{b}$	6100	$^{+3400}_{-3300}$	$^{+3300}_{-3200}$	$^{+700}_{-600}$	±300	±300	2040 ± 50
VH, $H \to \gamma\gamma$	5.0	$^{+2.6}_{-2.5}$	$^{+2.4}_{-2.2}$	$^{+1.0}_{-0.9}$	±0.5	±0.1	$4.54^{+0.13}_{-0.12}$
VH, $H \to ZZ^*$	36	$^{+63}_{-41}$	$^{+62}_{-41}$	$^{+5}_{-4}$	$^{+6}_{-4}$	$^{+4}_{-2}$	52.8 ± 1.4
VH, $H \to b\bar{b}$	1380	$^{+310}_{-290}$	$^{+210}_{-200}$	±150	$^{+120}_{-80}$	±140	1162^{+31}_{-29}
$t\bar{t}H$+tH, $H \to \gamma\gamma$	1.46	$^{+0.55}_{-0.47}$	$^{+0.48}_{-0.44}$	$^{+0.19}_{-0.15}$	$^{+0.17}_{-0.11}$	±0.03	$1.33^{+0.08}_{-0.11}$
$t\bar{t}H$+tH, $H \to VV^*$	212	$^{+84}_{-81}$	$^{+61}_{-59}$	$^{+47}_{-44}$	$^{+17}_{-10}$	$^{+31}_{-30}$	142^{+8}_{-12}
$t\bar{t}H$+tH, $H \to \tau\tau$	51	$^{+41}_{-35}$	$^{+31}_{-28}$	$^{+26}_{-21}$	$^{+6}_{-4}$	$^{+8}_{-6}$	$36.7^{+2.2}_{-3.1}$
$t\bar{t}H$+tH, $H \to b\bar{b}$	270	±200	±100	±80	$^{+40}_{-10}$	$^{+150}_{-160}$	341^{+20}_{-29}

ggF vs VBF

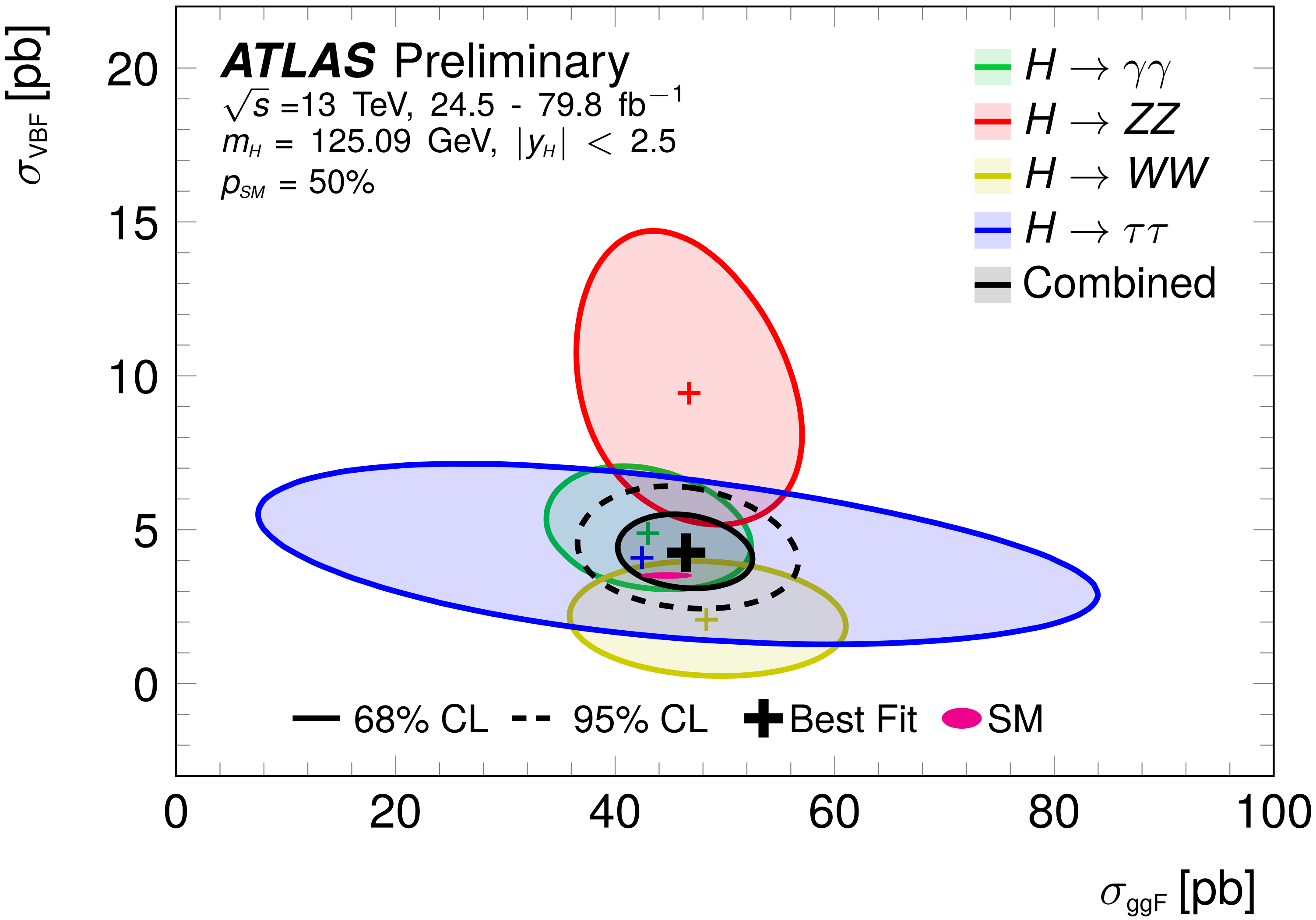

Figure 4: Observed likelihood contours in the plane of σ_{VBF} versus σ_{ggF} from individual channels and the combined fit. Contours for 68% (95%) CL, defined in the asymptotic approximation by $-2\ln\Lambda = 2.28$ (5.99), are shown in solid (dashed) lines. The crosses indicate the best-fit values, and the solid ellipse the SM prediction. Higgs boson branching fractions are fixed to their SM values within theory uncertainties. The compatibility between the combined measurement and the SM prediction, estimated using the procedure outlined in the text with 2 degrees of freedom, is indicated.

Correlation Matrix: Modes

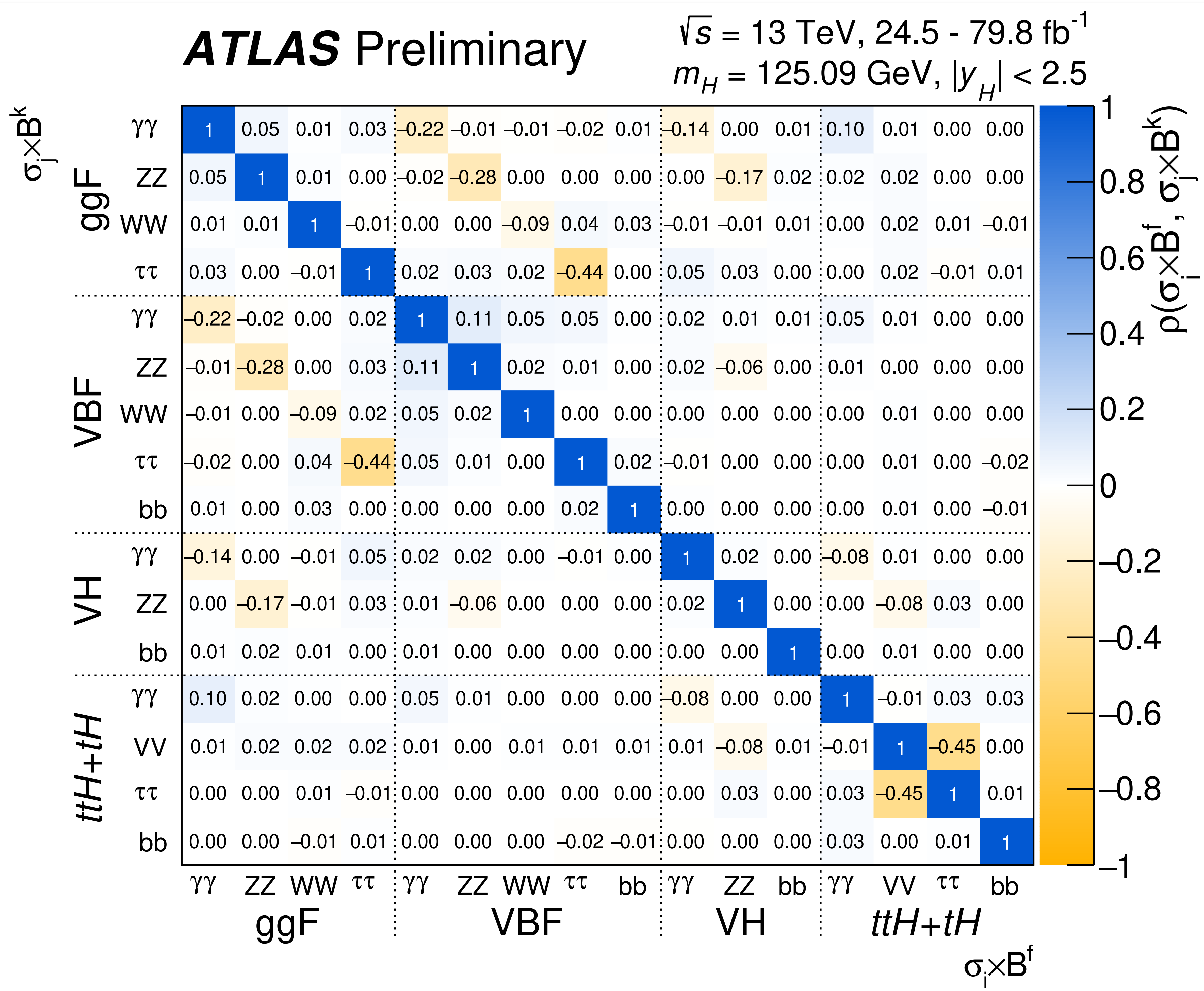

		ggF γγ	ggF ZZ	ggF WW	ggF ττ	VBF γγ	VBF ZZ	VBF WW	VBF ττ	VBF bb	VH γγ	VH ZZ	VH bb	ttH+tH γγ	ttH+tH VV	ttH+tH ττ	ttH+tH bb
ggF	γγ	1	0.05	0.01	0.03	−0.22	−0.01	−0.01	−0.02	0.01	−0.14	0.00	0.01	0.10	0.01	0.00	0.00
	ZZ	0.05	1	0.01	0.00	−0.02	−0.28	0.00	0.00	0.00	0.00	−0.17	0.02	0.02	0.02	0.00	0.00
	WW	0.01	0.01	1	−0.01	0.00	0.00	−0.09	0.04	0.03	−0.01	−0.01	0.01	0.00	0.02	0.01	−0.01
	ττ	0.03	0.00	−0.01	1	0.02	0.03	0.02	−0.44	0.00	0.05	0.03	0.00	0.00	0.02	−0.01	0.01
VBF	γγ	−0.22	−0.02	0.00	0.02	1	0.11	0.05	0.05	0.00	0.02	0.01	0.01	0.05	0.01	0.00	0.00
	ZZ	−0.01	−0.28	0.00	0.03	0.11	1	0.02	0.01	0.00	0.02	−0.06	0.00	0.01	0.00	0.00	0.00
	WW	−0.01	0.00	−0.09	0.02	0.05	0.02	1	0.00	0.00	0.00	0.00	0.00	0.00	0.01	0.00	0.00
	ττ	−0.02	0.00	0.04	−0.44	0.05	0.01	0.00	1	0.02	−0.01	0.00	0.00	0.00	0.01	0.00	−0.02
	bb	0.01	0.00	0.03	0.00	0.00	0.00	0.00	0.02	1	0.00	0.00	0.00	0.00	0.01	0.00	−0.01
VH	γγ	−0.14	0.00	−0.01	0.05	0.02	0.02	0.00	−0.01	0.00	1	0.02	0.00	−0.08	0.01	0.00	0.00
	ZZ	0.00	−0.17	−0.01	0.03	0.01	−0.06	0.00	0.00	0.00	0.02	1	0.00	0.00	−0.08	0.03	0.00
	bb	0.01	0.02	0.01	0.00	0.01	0.00	0.00	0.00	0.00	0.00	0.00	1	0.00	0.01	0.00	0.00
ttH+tH	γγ	0.10	0.02	0.00	0.00	0.05	0.01	0.00	0.00	0.00	−0.08	0.00	0.00	1	−0.01	0.03	0.03
	VV	0.01	0.02	0.02	0.02	0.01	0.00	0.01	0.01	0.01	0.01	−0.08	0.01	−0.01	1	−0.45	0.00
	ττ	0.00	0.00	0.01	−0.01	0.00	0.00	0.00	0.00	0.00	0.00	0.03	0.00	0.03	−0.45	1	0.01
	bb	0.00	0.00	−0.01	0.01	0.00	0.00	0.00	−0.02	−0.01	0.00	0.00	0.00	0.03	0.00	0.01	1

Figure 6: Correlation matrix for the measured values of the production cross sections times branching ratios of the Higgs boson, for the combinations in which sufficient sensitivity is provided by the input analyses.

Cross-section Ratios

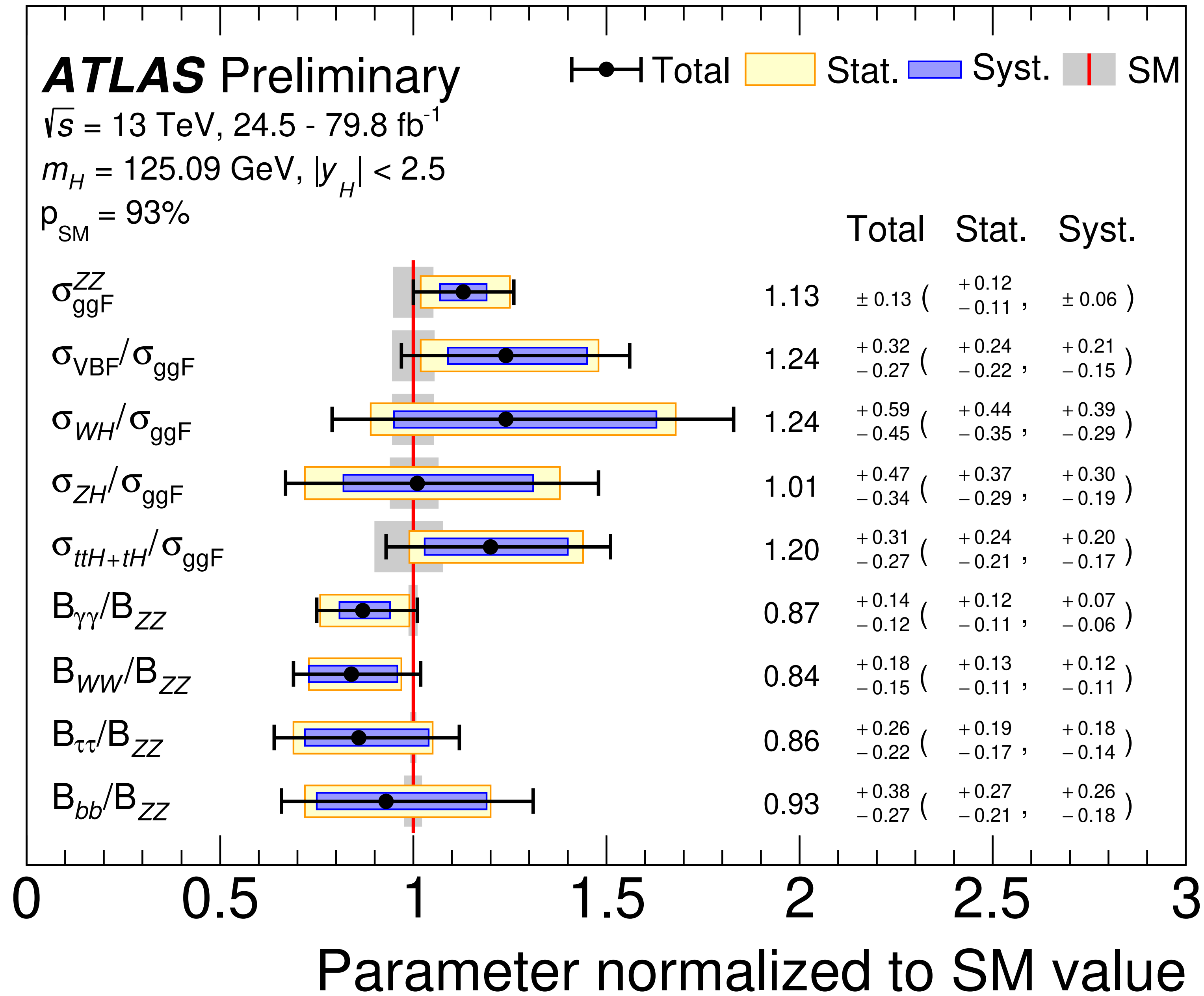

Figure 7: Results of a simultaneous fit for $\sigma^{ZZ}_{\mathrm{ggF}}$, $\sigma_{\mathrm{VBF}}/\sigma_{\mathrm{ggF}}$, $\sigma_{WH}/\sigma_{\mathrm{ggF}}$, $\sigma_{ZH}/\sigma_{\mathrm{ggF}}$, $\sigma_{t\bar{t}H+tH}/\sigma_{\mathrm{ggF}}$, $B_{\gamma\gamma}/B_{ZZ}$, B_{WW}/B_{ZZ}, $B_{\tau\tau}/B_{ZZ}$, and B_{bb}/B_{ZZ}. The fit results are normalized to the SM predictions. The black error bars, blue boxes and yellow boxes show the total, systematic, and statistical uncertainties in the measurements, respectively. The gray bands show the theory uncertainties in the predictions.

Cross-section Ratios (2)

Table 7: Best-fit values and uncertainties of $\sigma_{\mathrm{ggF}}^{ZZ}$, together with ratios of production cross sections normalized to σ_{ggF}, and ratios of branching fractions normalized to B_{ZZ}. Uncertainties in the SM predictions are computed following the same method as for Ref. [3].

Quantity	Value	Uncertainty					SM prediction
		Total	Stat.	Exp.	SigTheo.	BkgTheo.	
$\sigma_{\mathrm{ggF}}^{ZZ}$ [pb]	1.33	± 0.15	$^{+0.14}_{-0.13}$	± 0.06	± 0.02	± 0.04	1.181 ± 0.061
$\sigma_{\mathrm{VBF}}/\sigma_{\mathrm{ggF}}$	0.097	$^{+0.025}_{-0.021}$	$^{+0.019}_{-0.017}$	$^{+0.010}_{-0.008}$	$^{+0.011}_{-0.008}$	$^{+0.006}_{-0.005}$	0.0786 ± 0.0043
$\sigma_{WH}/\sigma_{\mathrm{ggF}}$	0.034	$^{+0.016}_{-0.012}$	$^{+0.012}_{-0.009}$	$^{+0.008}_{-0.006}$	$^{+0.003}_{-0.002}$	$^{+0.007}_{-0.005}$	$0.0269^{+0.0014}_{-0.0015}$
$\sigma_{ZH}/\sigma_{\mathrm{ggF}}$	0.0180	$^{+0.0084}_{-0.0062}$	$^{+0.0066}_{-0.0052}$	$^{+0.0034}_{-0.0021}$	$^{+0.0016}_{-0.0009}$	$^{+0.0037}_{-0.0025}$	$0.0178^{+0.0011}_{-0.0010}$
$\sigma_{t\bar{t}H+tH}/\sigma_{\mathrm{ggF}}$	0.0157	$^{+0.0041}_{-0.0035}$	$^{+0.0031}_{-0.0029}$	$^{+0.0020}_{-0.0017}$	$^{+0.0012}_{-0.0008}$	$^{+0.0013}_{-0.0012}$	$0.0131^{+0.0010}_{-0.0013}$
$\mathrm{B}_{\gamma\gamma}/\mathrm{B}_{ZZ}$	0.075	$^{+0.012}_{-0.010}$	$^{+0.010}_{-0.009}$	$^{+0.006}_{-0.005}$	$^{+0.002}_{-0.001}$	± 0.002	0.0860 ± 0.0010
$\mathrm{B}_{WW}/\mathrm{B}_{ZZ}$	6.8	$^{+1.5}_{-1.2}$	$^{+1.1}_{-0.9}$	$^{+0.8}_{-0.7}$	± 0.2	$^{+0.6}_{-0.5}$	$8.15 \pm < 0.01$
$\mathrm{B}_{\tau\tau}/\mathrm{B}_{ZZ}$	2.04	$^{+0.62}_{-0.52}$	$^{+0.45}_{-0.40}$	$^{+0.36}_{-0.31}$	$^{+0.17}_{-0.09}$	$^{+0.12}_{-0.09}$	2.369 ± 0.017
$\mathrm{B}_{bb}/\mathrm{B}_{ZZ}$	20.5	$^{+8.4}_{-6.2}$	$^{+6.2}_{-4.6}$	$^{+3.7}_{-2.4}$	$^{+1.3}_{-0.9}$	$^{+4.2}_{-2.9}$	22.00 ± 0.51

STXS in Combination

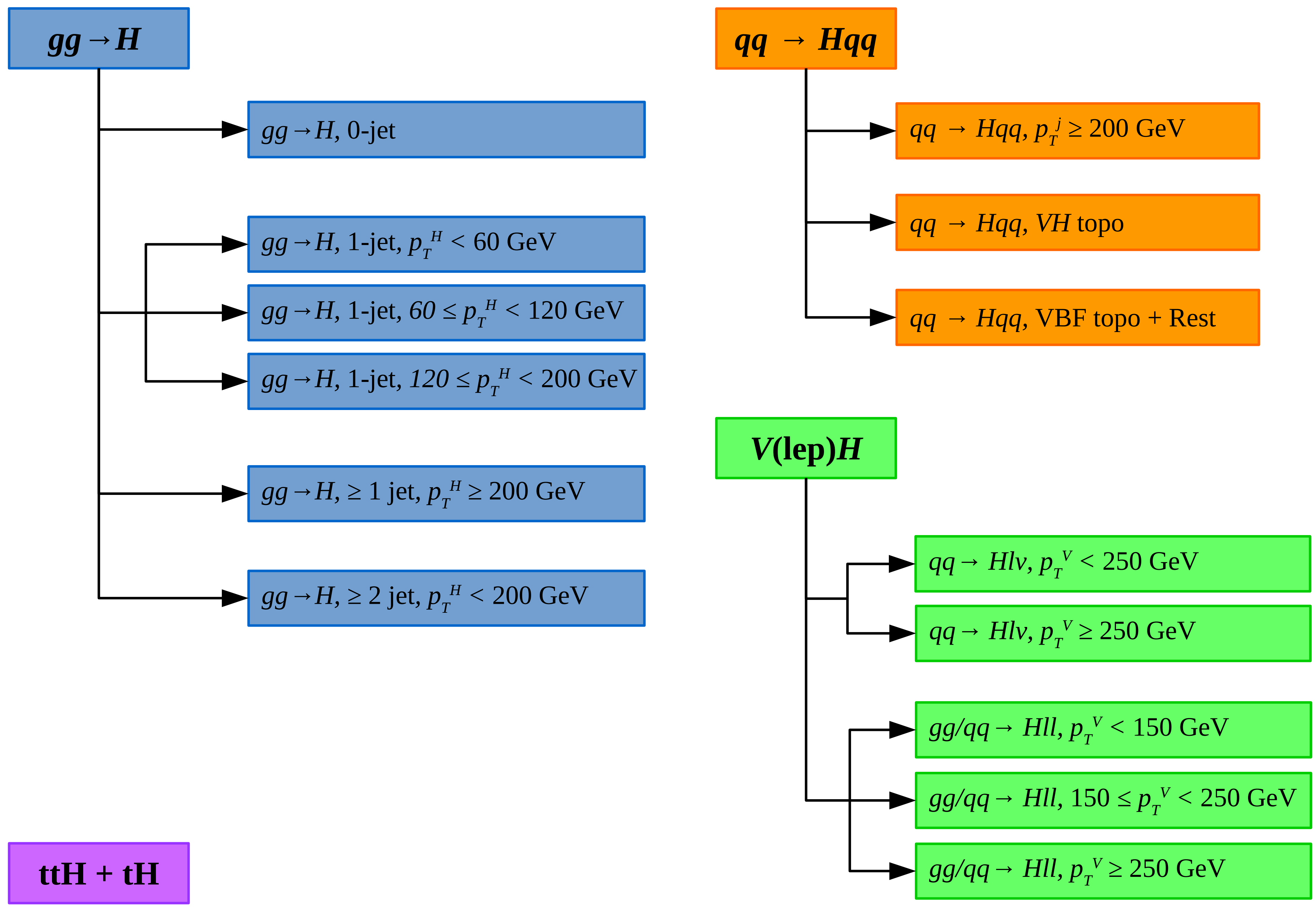

Figure 8: Definition of the STXS measurement regions used in this note. For each Higgs boson production process, the regions are defined starting from the top of the corresponding schematic, with regions nearer the top taking precedence in case of overlapping selections. The $b\bar{b}H$ production mode is considered as part of $gg \to H$.

κ_F vs κ_V

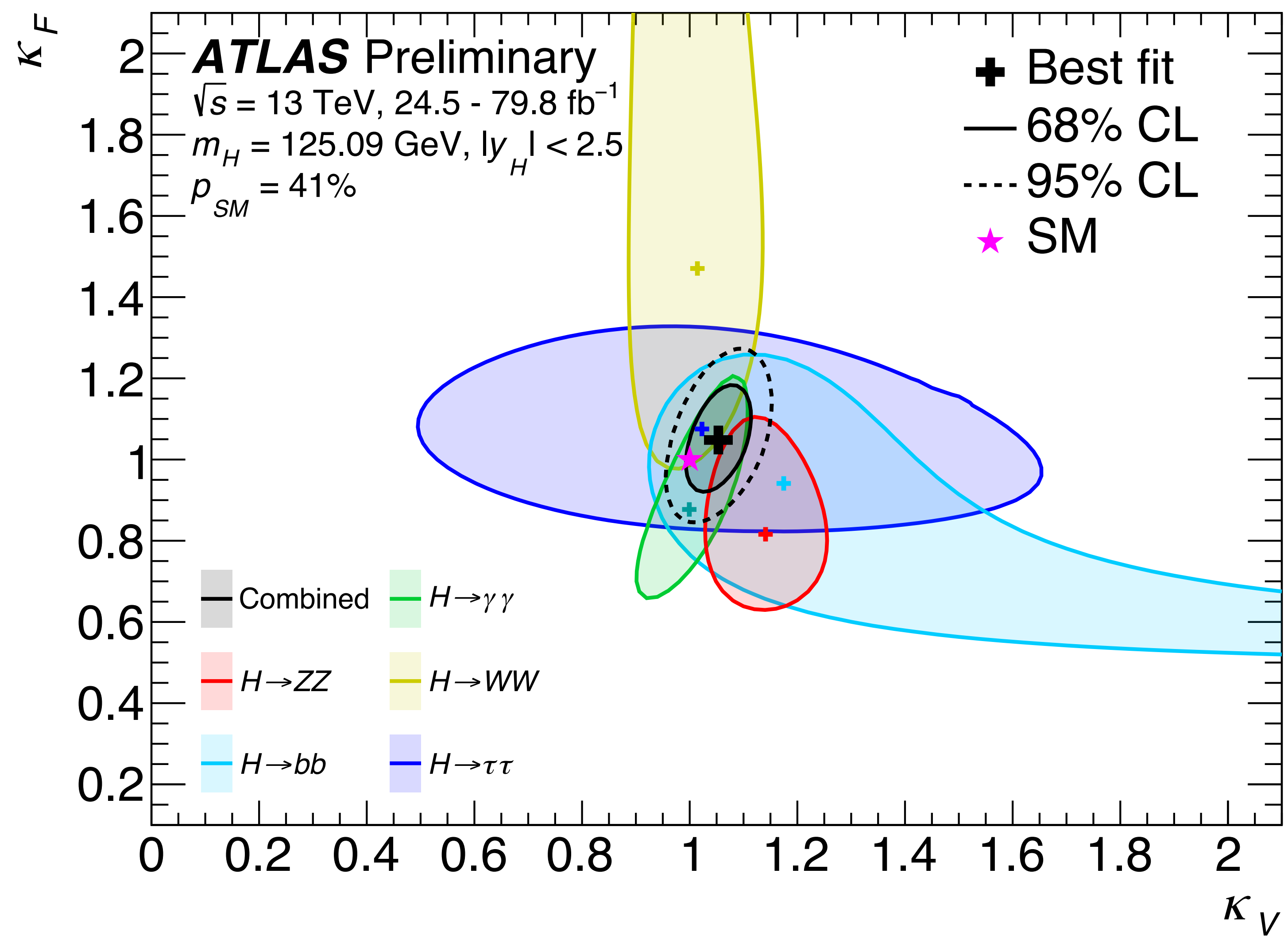

Figure 12: Negative log-likelihood contours at 68% and 95% CL in the (κ_V^f, κ_F^f) plane for the individual decay modes and their combination (κ_F versus κ_V shown in black) assuming the coupling strengths to fermions and vector bosons to be positive. No contributions from invisible or undetected Higgs boson decays are assumed. The best fit value for each measurement is indicated by a cross while the SM hypothesis is indicated by a star.

Generic Parametrisation

Table 12: Best-fit values and uncertainties of ratios of coupling modifiers. The second column provides the expression of the measured parameters in terms of the coupling modifiers defined in previous sections. All parameters are defined to be unity in the SM.

Parameter	Definition in terms of κ modifiers	Result
κ_{gZ}	$\kappa_g \kappa_Z / \kappa_H$	1.06 ± 0.07
λ_{tg}	κ_t / κ_g	$1.10^{+0.15}_{-0.14}$
λ_{Zg}	κ_Z / κ_g	$1.12^{+0.15}_{-0.13}$
λ_{WZ}	κ_W / κ_Z	0.95 ± 0.08
$\lambda_{\gamma Z}$	κ_γ / κ_Z	0.94 ± 0.07
$\lambda_{\tau Z}$	κ_τ / κ_Z	0.95 ± 0.13
λ_{bZ}	κ_b / κ_Z	$0.93^{+0.15}_{-0.13}$

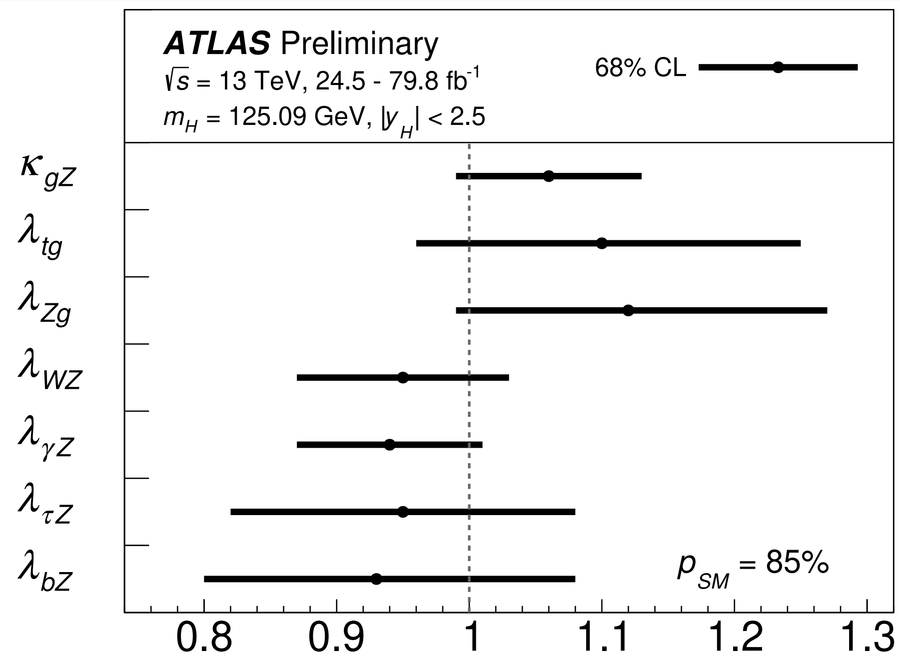

Figure 17: Measured ratios of coupling modifiers. The dashed line indicates the SM value of unity for each parameter.

Invisible Combination

Inputs

Table 1: Observed and expected upper limits on $\mathcal{B}_{H\to\text{inv}}$ at 95% CL from direct searches for invisible decays of the 125 GeV Higgs boson and statistical combinations. Also given are the observed p-values under the SM hypothesis.

Analysis	$\sqrt{s}$	Int. luminosity	Observed	Expected	p_{SM}-value	Reference
Run 2 VBF	13 TeV	36.1 fb^{-1}	0.37	$0.28^{+0.11}_{-0.08}$	0.19	[33]
Run 2 ZH	13 TeV	36.1 fb^{-1}	0.67	$0.39^{+0.17}_{-0.11}$	0.06	[34]
Run 2 VH	13 TeV	36.1 fb^{-1}	0.83	$0.58^{+0.23}_{-0.16}$	0.12	[35]
Run 2 Comb.	13 TeV	36.1 fb^{-1}	0.38	$0.21^{+0.08}_{-0.06}$	0.03	this note
Run 1 Comb.	7, 8 TeV	4.7, 20.3 fb^{-1}	0.25	$0.27^{+0.10}_{-0.08}$	—	[32]
Run 1+2 Comb.	7, 8, 13 TeV	4.7, 20.3, 36.1 fb^{-1}	0.26	$0.17^{+0.07}_{-0.05}$	0.10	this note

Additional Results

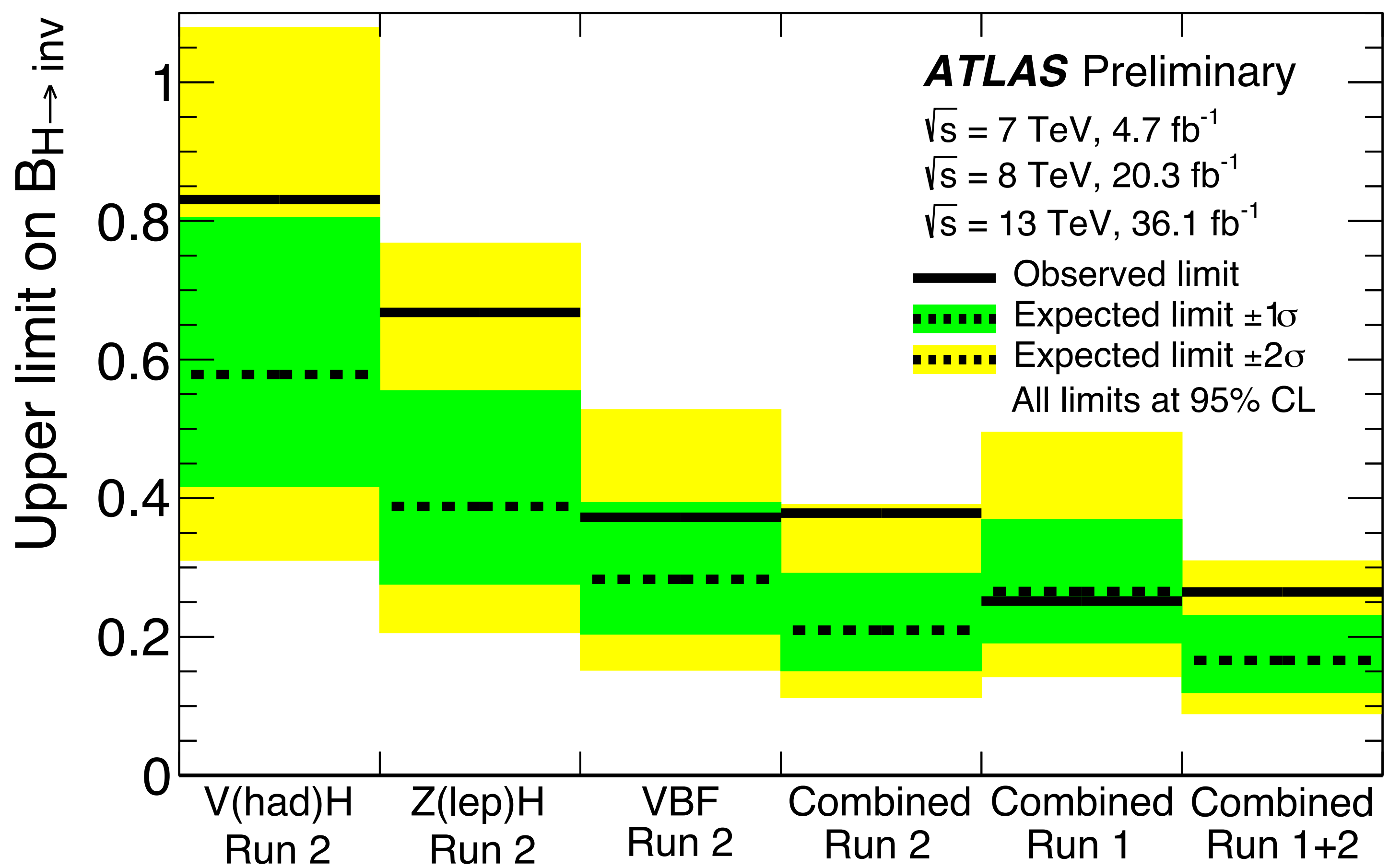

Figure 2: The observed and expected upper limits on $\mathcal{B}_{H\to\text{inv}}$ at 95% CL from direct searches for invisible decays of the 125 GeV Higgs boson and statistical combinations.